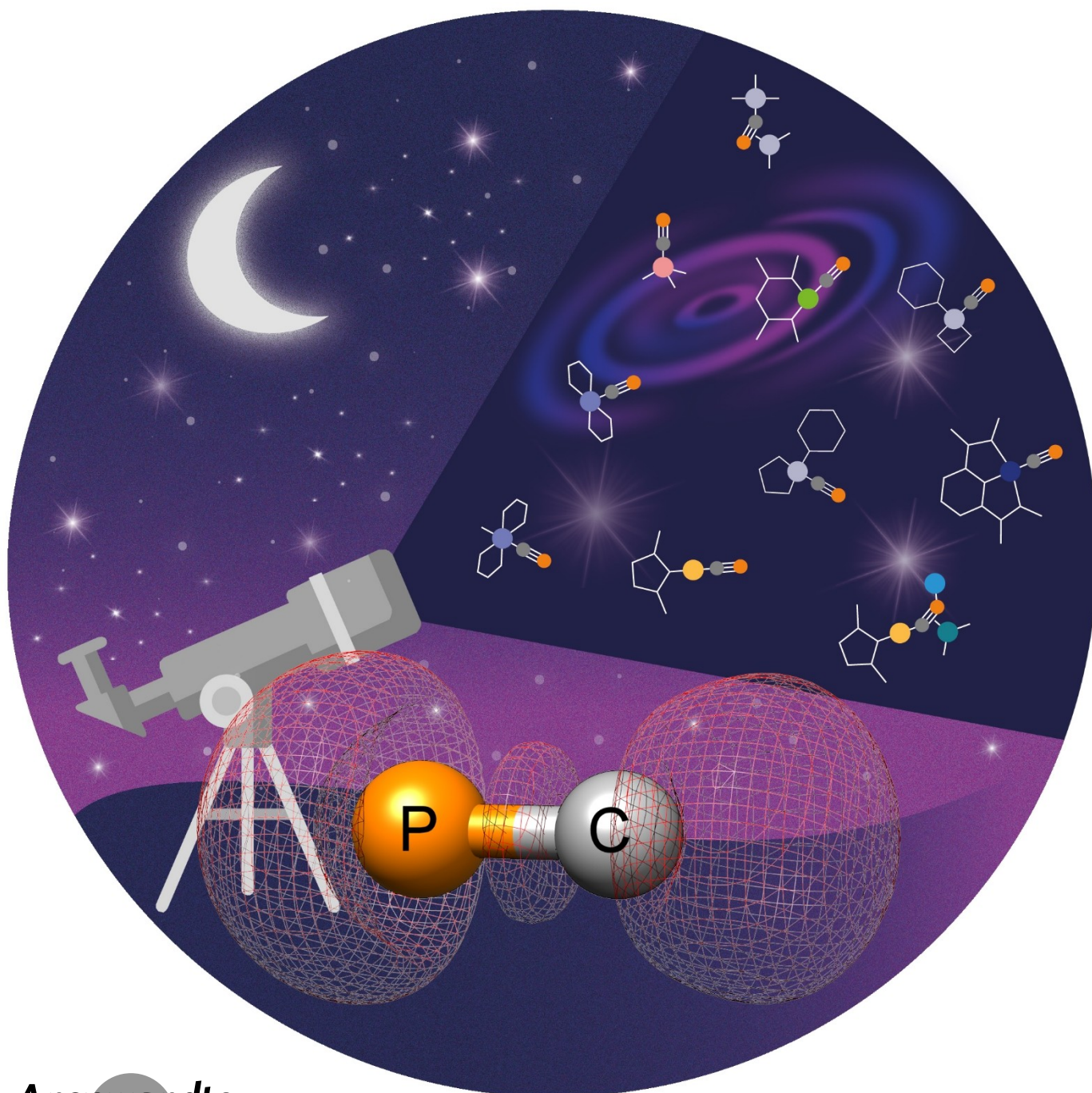


Main Group Elements

How to cite: *Angew. Chem. Int. Ed.* **2023**, *62*, e202217749
doi.org/10.1002/anie.202217749

The Chemistry of the Cyaphide Ion

Tim Görlich, Peter Coburger, Eric S. Yang, Jose M. Goicoechea,* Hansjörg Grützmacher,*
and Christian Müller*



Abstract: We review the known chemistry of the cyaphide ion, $(\text{C}\equiv\text{P})^-$. This remarkable diatomic anion has been the subject of study since the late nineteenth century, however its isolation and characterization eluded chemists for almost a hundred years. In this mini-review, we explore the pioneering synthetic experiments that first allowed for its isolation, as well as more recent developments demonstrating that cyaphide transfer is viable in well-established salt-metathesis protocols. The physical properties of the cyaphide ion are also explored in depth, allowing us to compare and contrast the chemistry of this ion with that of its lighter congener cyanide (an archetypal strong field ligand and important organic functional group). Recent studies show that the cyaphide ion has the potential to be used as a versatile chemical reagent for the synthesis of novel molecules and materials, hinting at many interesting future avenues of investigation.

1. Introduction

1.1. Historical Overview: The Cyaphide Ion

Low-coordinate phosphorus compounds have been the subject of study for over a century as researchers have sought to isolate phosphorus-containing analogs of unsaturated organic molecules. Historically, research in this area was largely driven by chemical curiosity, exploring and exploiting the isolobal relationship between a phosphorus atom and a methine moiety. Nowadays, many low coordinate phosphorus compounds such as phosphalkenes, phosphalkynes, aromatic phosphorus heterocycles, and phosphaketenes are commonly used in more applied research fields. They are, for instance, used as ligands in homogeneous catalysis, as precursors to phosphorus-containing materials, or as building blocks to previously inaccessible organophosphorus compounds.^[1–13] One relatively under-explored low-coordinate phosphorus species is the cyaphide ion $(\text{C}\equiv\text{P})^-$, the phosphorus analog of cyanide $(\text{C}\equiv\text{N})^-$, which has recently come to the fore as a promising chemical precursor. This review article will survey the known chemistry of this species and highlight future research opportunities using this simple, yet elusive, pseudo-halide ion.

[*] T. Görlich, Prof. Dr. C. Müller
Institut für Chemie und Biochemie, Freie Universität Berlin
Fabeckstr. 34/36, 14195 Berlin (Germany)
E-mail: c.mueller@fu-berlin.de

Dr. P. Coburger, Prof. Dr. H. Grützmacher
Department of Chemistry and Applied Biosciences, ETH Zürich
Vladimir-Prelog-Weg 1, 8093 Zürich (Switzerland)
E-mail: hgruetzmacher@ethz.ch

E. S. Yang, Prof. Dr. J. M. Goicoechea
Department of Chemistry, University of Oxford, Chemistry Research
Laboratory
12 Mansfield Rd., Oxford, OX1 3TA (UK)

Prof. Dr. J. M. Goicoechea
Department of Chemistry, Indiana University
800 East Kirkwood Ave., Bloomington, IN 47405 (USA)
E-mail: jgoicoec@iu.edu

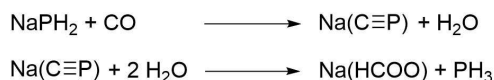
© 2023 The Authors. Angewandte Chemie International Edition published by Wiley-VCH GmbH. This is an open access article under the terms of the Creative Commons Attribution Non-Commercial License, which permits use, distribution and reproduction in any medium, provided the original work is properly cited and is not used for commercial purposes.

In contrast to more well-studied low-coordinate phosphorus compounds such as phosphalkynes (see below), the isolation of metal complexes of the cyaphide ion was only achieved relatively recently in 1992. The first attempted synthesis of the cyaphide ion, however, dates back to 1894 when Shoher and Spanutius claimed the synthesis of $\text{Na}(\text{C}\equiv\text{P})$ in a two-step reaction (Scheme 1). In their report, the reduction of PH_3 by elemental sodium was found to afford NaPH_2 , and/or the related species Na_2PH and Na_3P . Subsequent treatment with CO gas was believed to yield $\text{Na}(\text{C}\equiv\text{P})$ and H_2O . The authors postulated that the highly unstable $\text{Na}(\text{C}\equiv\text{P})$ salt immediately reacts with water, and the presence of sodium formate $\text{Na}(\text{HCOO})$ and phosphine (PH_3) in the decomposition products was considered as indirect proof of their theory.^[14]

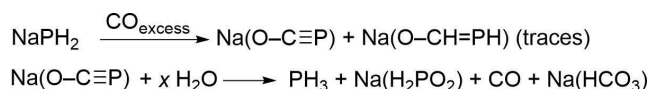
In 2011 (117 years later!), Grützmacher and co-workers reinvestigated the reactions of NaPH_2 with CO gas using modern analytical techniques.^[15] They found that instead of $\text{Na}(\text{C}\equiv\text{P})$, the product of the reaction was the sodium salt of the 2-phosphaethynolate ion, $(\text{O}-\text{C}\equiv\text{P})^-$, which was first characterized as the lithium salt by Becker in 1992 (Scheme 1).^[16] Despite many efforts over the course of the last hundred years, binary cyaphide salts still remain elusive.

In 1930, Herzberg was able to detect the vibrational spectrum of the $(\text{C}\equiv\text{P})^\bullet$ radical by setting off an electric discharge in a chamber filled with a mixture of argon and phosphorus vapor. The tap grease and/or the sealing wax may have introduced carbon to the electric arc, which permitted the formation of $(\text{C}\equiv\text{P})^\bullet$ radicals and potentially $(\text{C}\equiv\text{P})_2$, an analog of cyanogen. In accordance with this observation, a control experiment using argon and traces of dinitrogen revealed the typical bands for the $(\text{C}\equiv\text{N})^\bullet$ radical. This was the first reported generation of a cyaphide species,

Shoher & Spanutius (original claim, 1894)



Grützmacher et al. (2011)



Scheme 1. Reaction of NaPH_2 with CO . Top: proposed outcome (Shoher & Spanutius). Bottom: corroborated products (Grützmacher and co-workers).

although the resulting compound could not be isolated.^[17] Intriguingly, astronomers were later able to detect $(\text{C}\equiv\text{P})^\bullet$ radicals and even hydrogen cyaphide ($\text{H}-\text{C}\equiv\text{P}$) in outer space near the carbon- and oxygen-rich circumstellar envelopes of IRC +10216 and CRL 2688.^[18–20]

1.2. The Cyaphide Ion as a Functional Group: Phosphaalkynes

A major synthetic breakthrough was finally achieved in 1961, when Gier demonstrated the synthesis and isolation of $\text{H}-\text{C}\equiv\text{P}$ by passing PH_3 gas through a rotating arc between two graphite electrodes sealed in a water-cooled copper reactor. The gaseous products (hydrogen cyaphide,

acetylene, phosphine, and ethylene) were first condensed in cooling traps ($T = -196^\circ\text{C}$) then separated by gas-chromatography. The isolated $\text{H}-\text{C}\equiv\text{P}$ was characterized by elemental analysis, mass spectrometry, and infrared spectroscopy. Moreover, the reaction of $\text{H}-\text{C}\equiv\text{P}$ with anhydrous HCl resulted in the formation of $\text{CH}_3\text{P}(\text{Cl})_2$ as the sole product, giving further proof of its molecular composition.^[21] Further evidence for the existence of $\text{H}-\text{C}\equiv\text{P}$ was reported by Tyler who recorded its microwave spectrum.^[22] This was later corroborated by Nixon and co-workers, who observed the generation of $\text{H}-\text{C}\equiv\text{P}$ by dehydrohalogenation of dichloro-phosphines under flash vacuum pyrolysis conditions.^[23–25] The synthesis of $\text{H}-\text{C}\equiv\text{P}$ demonstrated the accessibility of compounds with carbon-phosphorus triple



Tim Görlich studied chemistry at the University of Würzburg interrupted by a temporarily stay at the University of Umeå (Sweden) to work on small heterocyclic anti-cancer agents under the supervision of Erik Chorell. He completed his master degree with the synthesis of new luminescent cationic rhodacyclopentadienes complexes under the guidance of Prof. Todd B. Marder. In 2018 he started his Ph.D. studies in the field of low-coordinated phosphorus compounds with focus on cyaphido complexes under the supervision of Prof. Christian Müller at Freie Universität Berlin.



Peter Coburger, year 1992, is a junior group leader at the TU Munich (Germany). His research interests are the coordination chemistry of redox-active π -ligands, especially cyclic biradicaloids, and the utilization of their main group and base metal complexes in catalysis and small molecule activation. He did his Ph.D. with Prof. Evamarie Hey-Hawkins (Leipzig University, 2015–2019) which was followed by postdoctoral research projects with Prof. Robert Wolf (Regensburg University, 2019–2020) and Prof. Hansjörg Grützmacher (ETH Zurich, 2020–2022).



Eric Yang received his M.Sci. from the University of Cambridge in 2019, where he studied main-group supramolecular chemistry under the supervision of Prof. D. Wright. He is currently at the University of Oxford as an Exonian scholar with the OxICFM CDT, completing his D.Phil. under the supervision of Prof. J. M. Goicoechea. His current research is on the synthesis of cyaphide-containing molecules and materials, with a particular focus on understanding the properties of the cyaphido ligand and investigating its reactivity.



Jose Goicoechea studied chemistry at the University of Zaragoza (Spain) and received his Ph.D. from the University of Bath (2003) under the supervision of Prof. Michael Whittlesey. Between 2003 and 2006 he was a PDRA with Prof. Slavi Sevov at the University of Notre Dame. In 2006 he was appointed as Lecturer at the University of Oxford and promoted to Full Professor in 2016. His research is primarily focused on the chemistry of Earth-abundant main-group elements. In January 2023 he will be joining the faculty of Indiana University, Bloomington.



Hansjörg Grützmacher studied Chemistry at the University of Göttingen and received their Ph.D. degree (1986) under the supervision of Prof. Dr. h.c. mult. H.W. Roesky. He joined the group of Prof. Guy Bertrand as chargé de recherche at the CNRS in Toulouse until end of 1987 and subsequently performed his habilitation until 1992 at the University of Heidelberg. He was appointed as Professor of Inorganic and Analytical Chemistry at the University of Freiburg (1992) before he joined the faculty at the Chemistry Department of the ETH Zürich first as extra-ordinary professor (1995) and since 2001 as full-professor (2001).



Christian Müller studied Chemistry at the University of Bielefeld and the University of Michigan (Ann Arbor) where he did a 9-month internship in the group of Prof. Arthur James Ashe III, working on aromatic boron-heterocycles. He received his Ph.D. degree from the University of Bielefeld (2000) under the supervision of Prof. Peter Jutzi. After two postdocs (University of Rochester with Prof. William D. Jones and University of Amsterdam with Prof. Piet van Leeuwen) he moved to Eindhoven University of Technology, where he started as an Assistant Professor. Since 2012 he is full professor of inorganic chemistry at Freie Universität Berlin, Germany.

bonds, paving the way for the synthesis of numerous phosphalkynes including the first thermally stable phosphalkyne, *t*Bu-C≡P, by Becker and co-workers in 1981.^[26,27] Phosphalkynes have since emerged as a well-studied class of compounds used as ligands and precursors in chemical synthesis.^[2,7,8]

With the demonstration that Pitzer's double bond rule was not applicable to phosphorus,^[28,29] the possibility of a stable (C≡P)⁻ anion began to be investigated theoretically.^[30] Its synthesis remained elusive until 1992, when the group of Angelici finally reported the first example of a coordination compound of the cyaphido ligand (see section 3.1).^[31]

2. C≡P⁻: Ligand Properties

2.1. Theoretical Studies and Spectroscopic Properties

Most analytical and theoretical studies on C≡P triple bonds focus on phosphalkynes.^[32–35] In comparison, the (C≡P)⁻ anion has been less extensively studied. This chapter will thus exclusively discuss the most important aspects of H-C≡P, the (C≡P)⁻ anion, and (C≡P)⁻ as a ligand.

Hydrogen cyaphide is a linear molecule and the phosphorus-containing analog of hydrocyanic acid (hydrogen cyanide). In contrast to H-C≡N, it is pyrophoric, highly reactive and polymerizes even at low temperatures. H-C≡P has been studied extensively using a variety of spectroscopic techniques including rotational-vibrational spectroscopy,^[36] Raman spectroscopy,^[37] microwave spectroscopy,^[22,38] and NMR spectroscopy.^[39] H-C≡P has also been studied theoretically in computational studies.^[40–42] The triple bond in H-C≡P (C^{δ-}≡P^{δ+}) is much less polarized than the C≡N triple bond in H-C≡N, due to the lower electronegativity of phosphorus compared to nitrogen.^[42]

Based on microwave spectroscopy the dipole moment of H-C≡P ($\mu(\text{H-C}\equiv\text{P})=0.39$ D) is much lower than that of hydrocyanic acid ($\mu(\text{H-C}\equiv\text{N})=3.00$ D). The H-C and C≡P bond lengths were found to be 1.067 Å and 1.540 Å, respectively (H-C≡N: 1.063 Å, 1.155 Å).^[22,43] Solid H-C≡P shows three main vibrational modes in its infrared spectrum, $\tilde{\nu}(\text{C-H stretch})=3120$ cm⁻¹, $\tilde{\nu}(\text{C}\equiv\text{P stretch})=1265$ cm⁻¹, and $\tilde{\nu}(\text{H-C-P bend})=671$ cm⁻¹ (cf. H-C≡N=3180, 2120, 830 cm⁻¹).^[21] The ³¹P NMR spectrum of H-C≡P reveals a resonance at $\delta(^{31}\text{P})=-32.0$ ppm (d, ²J_{P-H}=43.9 Hz), while the ¹³C NMR spectrum shows a single resonance at $\delta(^{13}\text{C})=154$ ppm (dd, ¹J_{C-H}=211 Hz, ¹J_{C-P}=54.0 Hz).^[39] As expected, calculations on the gas-phase acidity (ΔG^0_{acid}) reveals that H-C≡P is a weaker Brønsted acid than H-C≡N.^[44]

Based on calculations, the dipole moment of the (C≡P)⁻ anion is strongly increased to 2.42 D compared to H-C≡P,^[45] whereby most of the partial negative charge is located on the carbon atom (-0.83 at C, -0.17 at P). The partial charge on the phosphorus atom generally decreases upon coordination to a metal center.^[42] Calculations also provide insight into the distribution of the 10 valence electrons (VE). In (C≡P)⁻, they are shared between the carbon atom (2.66 VE), the phosphorus atom (4.22 VE) and the corresponding

C-P bond (2.91 VE). In (C≡N)⁻, there is greater electron density in the C-N bond (3.54 VE) and the carbon atom (2.86 VE), with fewer electrons on the nitrogen atom (3.39 VE).

According to calculations, the C-P bond length in the (C≡P)⁻ anion is 1.598 Å (cf. (C≡N)⁻=1.180 Å due to the smaller covalent radius of nitrogen), in contrast to the values of approximately 1.54 Å found experimentally for phosphalkynes, and 1.56 Å for transition metal complexes containing terminal cyaphido ligands. The calculated harmonic vibrational stretching frequency for (C≡P)⁻ is $\tilde{\nu}=1198$ cm⁻¹ (cf. (C≡N)⁻: $\tilde{\nu}=2108$ cm⁻¹), while ΔH^0 for the formation of (C≡P)⁻ was found to be higher in comparison to C≡N⁻. This suggests that the cyaphide anion is less stable than its congener, the ubiquitous cyanide ion.^[30,42,44]

2.2. Coordination Modes

We have performed additional density functional theory (DFT) calculations to provide insight into the frontier orbitals of the cyaphido ligand with respect to the well-established cyanido ligand.^[46] The MO Scheme (Figure 1) reveals similar energies for the HOMOs, indicating that both the cyaphido and the cyanido ligand possess similar σ -donor strengths, once coordinated to a metal center via the carbon atom. In contrast, the degenerate LUMO/LUMO+1 of (C≡P)⁻ are energetically stabilized by 3 eV. Further, the degenerate HOMO-1/HOMO-2 are destabilized by 0.6 eV in the cyaphide anion. Since these two orbital sets correspond to π^* and π orbitals, respectively, the chemistry of the cyaphide anion is dominated by the π -manifold, with slightly better net-donor and much stronger π -acceptor ligand properties than the cyanide anion.

The calculated CO-stretching frequencies ($\tilde{\nu}_{(\text{CO})}$) of the generic nickelates [Ni(CO)₃(η^1 -C≡E)]⁻ (E=N, P) are depicted in Figure 2. The lower $\tilde{\nu}_{(\text{CO})}$ values found for the cyaphido complexes indicate a greater degree of electron

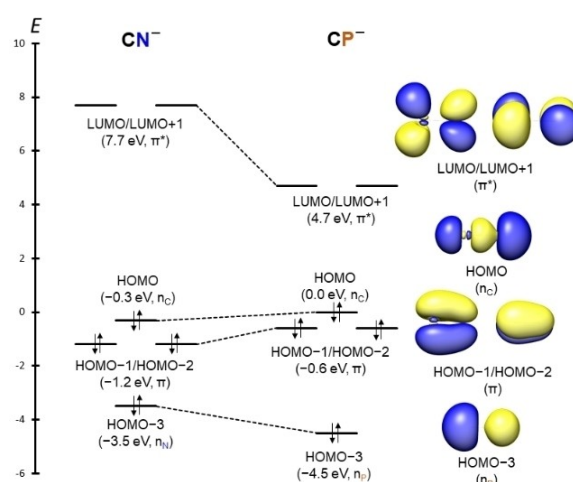


Figure 1. Frontier orbital energy levels of (C≡N)⁻ and (C≡P)⁻ (left) and selected MOs of (C≡P)⁻ (right).

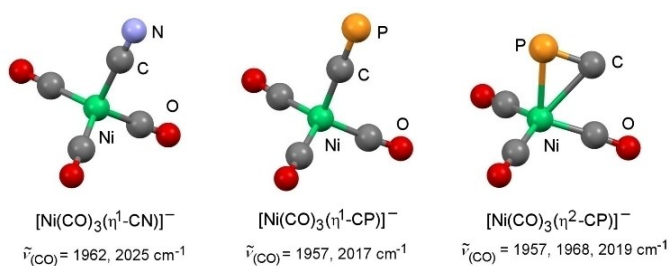


Figure 2. Calculated structures of the generic nickelates $[\text{Ni}(\text{CO})_3(\eta^1\text{-C}\equiv\text{E})]^-$ ($\text{E} = \text{N}, \text{P}$) and their CO-stretching frequencies.

density at the metal center (and concomitantly stronger electron back-donation into the $\pi^*(\text{CO})$ -orbitals), which point to slightly higher net-donor properties of $(\text{C}\equiv\text{P})^-$. The calculated C–P distance in $[\text{Ni}(\text{CO})_3(\eta^1\text{-C}\equiv\text{P})]^-$ is 1.582 Å, which is shorter than the distance found in the calculated cyaphide anion (1.607 Å). This suggests little to no metal-to-ligand back-bonding to the cyaphido ligand.

Interestingly, a second minimum structure for $[\text{Ni}(\text{CO})_3(\eta^1\text{-C}\equiv\text{P})]^-$ was found, where the cyaphide anion is coordinated in a side-on fashion to the nickel(0) atom, $[\text{Ni}(\text{CO})_3(\eta^2\text{-C}\equiv\text{P})]^-$ (Figure 2). This isomer is higher in energy than the σ -coordinated nickelate (energy difference $\Delta E = 20.9 \text{ kcal}\cdot\text{mol}^{-1}$), while the calculated $\tilde{\nu}_{(\text{CO})}$ values are very

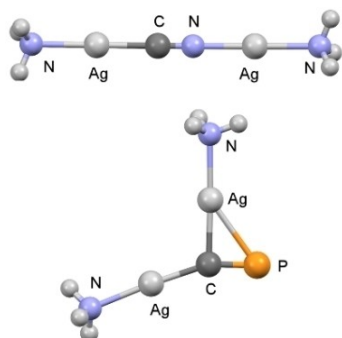


Figure 3. Linear bridging mode of the cyanido ligand in $[(\text{Ag}(\text{NH}_3)_2\{\mu\text{-}\eta^1:\eta^1\text{-C}\equiv\text{N}\})]^+$ (top) and σ - and π -coordination of the cyaphido ligand in $[(\text{Ag}(\text{NH}_3)_2\{\mu\text{-}\eta^1:\eta^2\text{-C}\equiv\text{P}\})]^+$ (bottom).

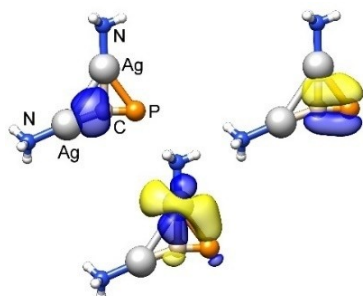


Figure 4. NOCVs corresponding to σ -donating (top) and π -accepting (bottom) interactions between the cyaphido ligand and silver ammine fragments in $[(\text{Ag}(\text{NH}_3)_2\{\mu\text{-}\eta^1:\eta^2\text{-C}\equiv\text{P}\})]^+$.

similar to those for $[\text{Ni}(\text{CO})_3(\eta^1\text{-C}\equiv\text{P})]^-$. Due to the π -coordination, the C–P bond length in $[(\text{Ni}(\text{CO})_3(\eta^2\text{-C}\equiv\text{P}))]^-$ increases to 1.622 Å. The π -coordination mode leads to the minimum energy structure of the homobimetallic complex $[(\text{Ag}(\text{NH}_3)_2\{\mu\text{-}\eta^1:\eta^2\text{-C}\equiv\text{P}\})]^+$. While the analogous cyanido complex $[(\text{Ag}(\text{NH}_3)_2\{\mu\text{-}\eta^1:\eta^1\text{-C}\equiv\text{N}\})]^+$ shows a linear bridging mode of the central cyanido ligand.

In $[(\text{Ag}(\text{NH}_3)_2\{\mu\text{-}\eta^1:\eta^2\text{-C}\equiv\text{P}\})]^+$ the cyaphide anion binds to one silver atom via the carbon atom (σ -coordination, Ag–C: 2.001 Å), whereas a second silver atom is bound via the π -manifold (Ag–C 2.138 Å, Ag–P 2.651 Å, Figure 3 and 4). Energy decomposition analysis in combination with natural orbital for chemical valence calculations (EDA-NOCV) show that the cyaphido ligand acts simultaneously as a σ -donor (via the C-atom and via one π_{CP} -orbital; $25.3 \text{ kcal}\cdot\text{mol}^{-1}$) and π -accepting ligand ($12.8 \text{ kcal}\cdot\text{mol}^{-1}$) in this complex. This is in line with the rather small energy gap between the HOMO–1/HOMO–2 and the LUMO/LUMO + 1 orbitals in $(\text{C}\equiv\text{P})^-$ (4.7 eV, Figure 1).

When the two $[\text{Ag}(\text{NH}_3)]^+$ fragments are formally replaced by $[\text{Ru}^{\text{II}}(\text{NH}_3)_5]^{2+}$ and $[\text{Ru}^{\text{III}}(\text{NH}_3)_5]^{3+}$, dinuclear paramagnetic complexes are obtained, which allow the influence of the bridging $\text{C}\equiv\text{E}$ ligand ($\text{E} = \text{N}, \text{P}$) on the structure of the electronic ground state to be investigated. Interestingly, the cyanido complex $[\text{Ru}^{\text{II}}(\text{NH}_3)_5\{\mu\text{-}\eta^1:\eta^1\text{-C}\equiv\text{N}\} \text{Ru}^{\text{III}}(\text{NH}_3)_5]^{4+}$ retains its linear M–C≡N–M structure (Figure 5). The $(\text{C}\equiv\text{P})^-$ ligand in the analogous cyaphido complex also adopts a σ -bridging mode, however in a zig-zag fashion (Ru–C–P: 158.0° , C–P–Ru: 144.0° , C–P: 1.664 Å, Figure 5). Not only do the structures of these two complexes deviate from each other, their electronic structures also show some profound differences. In the cyanido complex, the spin-population is exclusively located on the formal ruthenium(III)-fragment, which coordinates to the lone pair of the nitrogen atom. In contrast, the spin-population in the cyaphido complex is rather evenly distributed over the whole molecule (Ru: 0.4 each, $(\text{C}\equiv\text{P})^-$: 0.2). Therefore, the cyanido complex can be described as a ruthenium(II)-ruthenium(III) complex, whereas the corresponding cyaphido complex is best described as a mixed-valent complex in

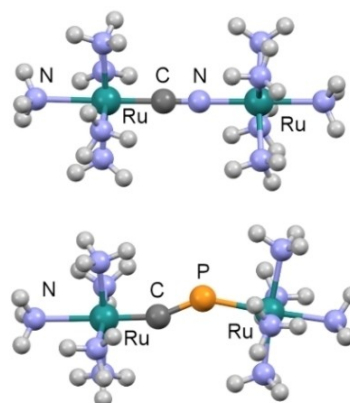


Figure 5. Cyanido complex $[\text{Ru}^{\text{II}}(\text{NH}_3)_5\{\mu\text{-}\eta^1:\eta^1\text{-C}\equiv\text{N}\} \text{Ru}^{\text{III}}(\text{NH}_3)_5]^{4+}$ (top) with a linear M–C≡N–M structure and the analogous cyaphido complex with a σ -bridging mode in a zig-zag fashion (bottom).

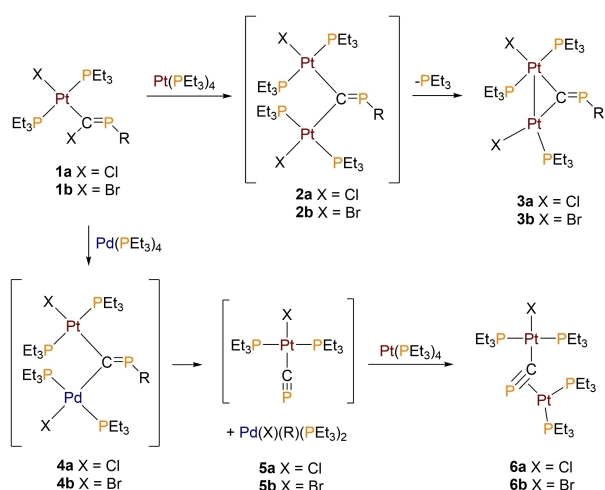
which each ruthenium center formally has a formal oxidation state of +2.5.

In summary, our calculations show that the cyaphide anion is not only a fundamental curiosity, but also has the potential to be used for the synthesis of metal complexes with markedly different structural and electronic properties than the corresponding cyanido complexes. While one metal fragment can apparently form the terminal σ -complex $[M]-C\equiv P$, a second one may interact in a side-on η^2 -fashion with the $C\equiv P$ triple bond. This coordination mode is driven by the energetically low-lying π^* orbitals of the $C\equiv P$ ligand, into which the metal fragment $[M']$ donates electron density. For simplicity reasons, we will refer to this terminal/side-on arrangement as an $\eta^1:\eta^2$ coordination mode [formally $\mu-(M')\eta^2-(C\equiv E)-(M)\kappa C$]. The alternative linear $\eta^1:\eta^1$ coordination mode [formally $\mu-(C\equiv E)-(M)\kappa C:(M')\kappa E$] would be the more classical end-on/end-on bridging mode, as usually observed for the cyanido ligand. In case of the cyaphido ligand, however, a *trans* bent $\eta^1:\eta^1$ arrangement will be formed when steric interactions do not allow the $\eta^1:\eta^2$ coordination mode. Details on the synthesis of multi-metallic complexes containing bridging cyaphido ligands (which further corroborate these computational results) are explicitly described in Sections 3 and 5.

3. $(C\equiv P)^-$: Synthesis

3.1. Generation of $(C\equiv P)^-$ from a bridging $\mu-C=P-R$ ligand

In 1991 Angelici reported on the synthesis of bimetallic platinum complexes bearing a bridging isocyaphide ligand ($C=P-R$; **3a/b**, Scheme 2).^[47] That same year, Weber also reported on the synthesis of related iron complexes.^[48] Treatment of the phosphavinyl platinum complexes *trans*- $[(X)(PEt_3)_2Pt(\kappa C-C(X)=PR)]$ (**1a/b**; X = Cl, Br; R = 2,4,6-*tert*-butylphenyl) with 1 equiv of $[Pt(PEt_3)_4]$ resulted in



Scheme 2. Reaction pathways for the synthesis of the diplatinum complexes **3a/b** and the cyaphido bridged complexes $[(X)(PEt_3)_2Pt((\mu-\eta^1:\eta^2-C\equiv P)Pt(PEt_3)_2)]$ (**6a/b**); R = 2,4,6-*tert*-butylphenyl.

the formation of the air-stable dinuclear complexes $[(X)(PEt_3)Pt(\mu_2-C=P-R)Pt(PEt_3)_2(X)]$ (**3a/b**), bearing a μ_2 -bridging isocyaphide moiety (Scheme 2).

The coordination compounds **2a/b** are presumed intermediates in this reaction, which are formed after the initial oxidative addition of the C–X bond of **1a/b** to $[Pt(PEt_3)_4]$. Addition of $[Pd(PEt_3)_4]$ to **1a/b** afforded the mixed intermediates **4a/b**, which, astonishingly, reacted further to afford a mixture of *trans*- $[(X)(PEt_3)_2Pd(R)]$ and the first ever reported terminal cyaphido complexes *trans*- $[(X)(PEt_3)_2Pt-(C\equiv P)]$ (**5a/b**). These are formed by a transfer of the aryl substituent (R) from the phosphorus atom of the bridging isocyaphide ligand to the palladium fragment, accompanied by the scission of a C–Pd bond. The formed coordination compounds are remarkably stable in non-polar organic solvents but all attempts to separate $[(X)(PEt_3)_2Pd(R)]$ from **5a/b** failed. However, the cyaphido complexes could be analyzed by means of NMR spectroscopy, which revealed a triplet resonance in the $^{31}P\{^1H\}$ NMR spectrum at $\delta=68.0$ ppm for the cyaphide phosphorus nucleus with a $^3J_{P-P}$ coupling constant of 9.2 Hz and an additional $^2J_{P-Pt}$ coupling of 303 Hz. Furthermore, **5a/b** were successfully reacted with a second equivalent of $[Pt(PEt_3)_4]$ yielding the cyaphido bridging complexes $[(X)(PEt_3)_2Pt(\eta^1:\eta^2-C\equiv P)Pt(PEt_3)_2]$ (**6a/b**), which could be fully characterized by means of NMR spectroscopy, elemental analysis, and single crystal X-ray diffraction to unambiguously verify the proposed structure (Figure 6).

Although complex **6a/b** does not contain a terminal cyaphido ligand due to the side-on coordination of an additional $[Pt(PEt_3)_2]$ fragment, DFT calculations still suggest the presence of a $P\equiv C$ triple bond.^[42] The resonance of the phosphorus atom of the bridging cyaphido ligand in **6a/b** appears as a doublet of doublet of triplets at $\delta=107.0$ ppm in the $^{31}P\{^1H\}$ NMR spectrum. The triplet arises from the two PEt_3 co-ligands at the $[(X)Pt^II(C\equiv P)]$ core, whereas the two doublets are caused by the two magnetically inequivalent PEt_3 co-ligands at the π -coordinated platinum(0) fragment. Two additional ^{195}Pt satellites are observed with coupling constants of $^2J_{Pt(\eta^1-CP)-P}=255$ Hz and $^1J_{Pt(\eta^2-CP)-P}=58$ Hz. The solid-state structures of **6a/b** clearly show that the two Pt centers are not bonded to one another.

The $C\equiv P$ bond length of 1.666(6) Å in **6a** is longer than the average $C\equiv P$ distance of an uncoordinated phosphalkyne (1.54 Å) and the calculated $C\equiv P$ bond length of the

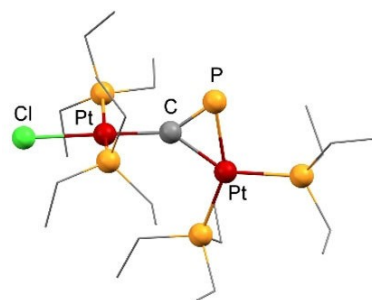


Figure 6. Solid-state molecular structure of **6a**.

terminal cyaphido ligand (1.566 Å) in complex **4a**. Moreover, the Pt–C≡P bond-angle of 144.0(3)° in **6a** significantly deviates from linearity.^[31,49] In summary, complexes **6a/b** were the first examples of authenticated dinuclear cyaphide complexes in which the C≡P ligand adopts a η¹:η²-coordination mode, which is in keeping with the theoretical predictions in section 2.2.

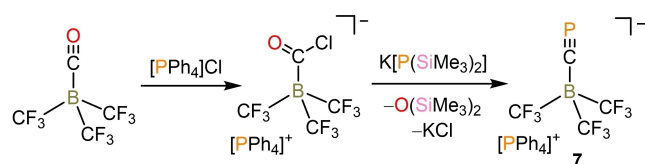
3.2. Generation of (C≡P)[−] by elimination of Me₃Si–O–SiMe₃

In 2004 Willner and co-workers reported the first successful isolation of a cyaphido borate salt. In this compound, the cyaphide ion acts as a Lewis base and forms a donor-acceptor adduct with B(CF₃)₃. The synthesis of this compound followed the typical elimination route used for the preparation of phosphalkynes, namely the elimination of Me₃Si–O–SiMe₃ from an acyl-halide using potassium bis(trimethylsilyl)phosphide, which results in the formation of a C≡P triple bond (Scheme 3).^[8]

The resulting cyaphido borate anion [(CF₃)₃B(η¹-C≡P)][−] was isolated as a colorless tetraphenyl phosphonium salt (**7**) which has a melting point of *T* = 125 °C. The C≡P moiety of **7** showed resonances at δ(¹³C) = 202.3 ppm and δ(³¹P) = 39.6 ppm in the corresponding NMR spectra. The Raman spectrum showed a C≡P stretching band at $\tilde{\nu}$ = 1468 cm^{−1}, while the solid-state structure revealed a C≡P distance of 1.563(10) Å. Interestingly, **7** was remarkably stable in the presence of moisture, likely due to the Coulombic stability afforded by the anionic charge of the cyaphido borate ion.^[50]

3.3. Generation of C≡P[−] by deprotection of silyl phosphalkynes

An often-used route for the generation of metal cyaphido complexes involves the deprotection of coordinated silyl phosphalkynes. Phosphalkynes overwhelmingly prefer coordination to metal centers in side-on η² modes, with very few examples of end-on η¹ coordination via the phosphorus lone pair.^[51,52] This rare coordination mode, however, enabled the generation of the cyaphide ligand as reported by Cordaro, Grützmacher and co-workers, who used a kinetically stabilized phosphalkyne with an adequate leaving group. At the ionic extreme of the bonding continuum, triphenylmethyl phosphalkyne can be viewed as a Lewis acid-base adduct of the (triphenyl)methyl cation and the cyaphide anion, i.e. Ph₃C^{δ+}(C≡P)^{δ−}. Attempts at treating η¹ metal complexes of this phosphalkyne [MH(dppe)₂(η¹-P≡C–CPh₃)]OTf (M = Fe, Ru, dppe = 1,2-bis(diphenylphosphino)ethane) with nucleophiles to afford



Scheme 3. Synthesis of [PPh₄][(CF₃)₃B(η¹-C≡P)] (**7**).

cyaphido metal complexes were unsuccessful, presumably due to the presence of a strong, non-polar C–C bond. However, when the same strategy was applied to metal complexes of the silylphosphalkyne Ph₃Si–C≡P [δ(³¹P) = 111.0, δ(¹³C) = 193.3 ppm (d, ¹J_{C-P} = 16.4 Hz)], cleavage of the more reactive Si–C bond enabled access to terminal cyaphido complexes. Although Ph₃Si–C≡P cannot be isolated and is kinetically and thermodynamically unstable (*t*_{1/2} ≈ 1 d at *T* = 23 °C), it can be isolated as an η¹-coordinated ligand in the complex [RuH(dppe)₂(η¹-P≡C–SiPh₃)] [OTf]. This was proven by means of NMR spectroscopy [δ(³¹P) = 143.8 ppm (d, ²J_{P-P} = 27.8 Hz), δ(¹³C) = 175.1 ppm (*J*_{C-P} = 71.4 Hz)], as well as by single crystal X-ray diffraction (P≡C bond length: 1.530(3) Å). The addition of a slight excess of sodium phenoxide lead to cleavage of the Si–C bond and generation of the first isolable metal complex containing a terminal cyaphido ligand, [RuH(η¹-C≡P)(dppe)₂] (**8**). The ³¹P NMR spectrum of **8** revealed a broadened resonance at δ(³¹P) = 143.8 ppm, which shows coupling to the hydride (d, ³J_{P-H} = 19.5 Hz). The quaternary carbon atom of the (C≡P)[−] ligand was detected in a ¹³C-¹H HMQC experiment and shows a resonance at 287.1 ppm (¹J_{P-C} ≈ 90 Hz). [RuH(η¹-C≡P)(dppe)₂] is only moderately air-sensitive in the solid state. The molecular structure was determined by means of single-crystal X-ray crystallography (Figure 7). The C≡P distance of 1.573(2) Å is longer than in free phosphalkynes, but much shorter than in side-on coordinated phosphalkyne complexes and in η¹:η² bridging cyaphido complexes. The Raman and infrared spectra displayed intense bands at $\tilde{\nu}$ = 1229 cm^{−1} corresponding to the C≡P vibrational mode.^[53]

A possible minimum energy reaction pathway for this transformation was calculated using DFT on truncated model complexes. There is experimental evidence that a nucleophile (e.g. MeO[−]) attacks reversibly at the phosphorus atom of the coordinated silylated phosphalkyne in **A** to give **B** (Scheme 4). Likely, **B** is also in equilibrium with the C-metallated phosphalkene **C**, which may form from **B** via a 1,2-shift of the metal fragment in a slightly exothermic reaction. However, according to DFT calculations, elimination of H₃Si–O–CH₃ from **C** to directly give the cyaphido complex **H** would proceed via an energetically inaccessible transition state (Δ*H* = 38 kcal·mol^{−1}). Instead, a more plausible reaction pathway involves the attack

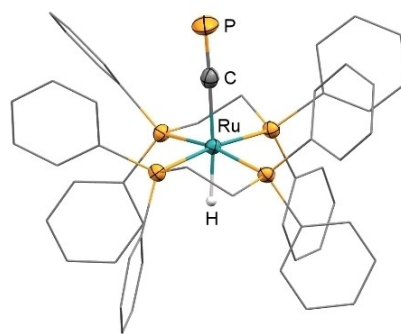
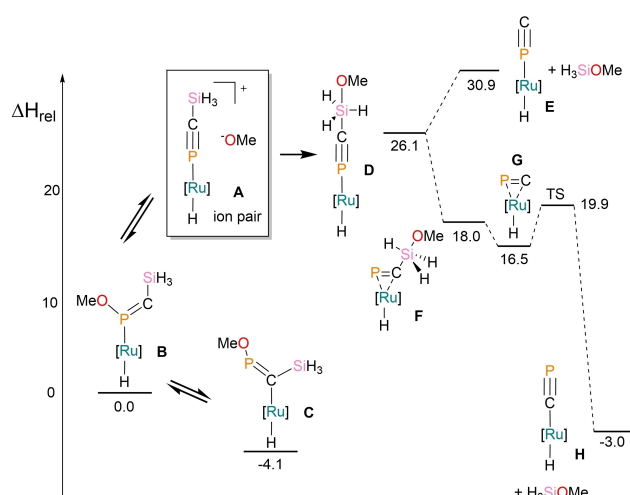


Figure 7. Solid-state molecular structure of **8**.



Scheme 4. Calculated reaction pathway (DFT) for the formation of the cyaphido complex **H**. The calculations were performed with $[\text{Ru}] = [\text{Ru}(\text{PH}_3)_4]$ and the simplified phosphalkyne $\text{H}_3\text{Si}-\text{C}\equiv\text{P}$.

of the methoxide at the silicon center of **A** to give **D**. This species rearranges immediately to complex **F**, which contains a side-on coordinated $[(\text{MeO})\text{H}_3\text{Si}-\text{C}\equiv\text{P}]^-$ -ligand. Subsequently, H_3SiOMe is eliminated to afford the complex **G** with a side-on coordinated $\text{C}\equiv\text{P}^-$ ligand that rotates to give the final product **H**. The rotation proceeds via a small energy barrier (TS) of $\Delta H = 3.4$ kcal $\cdot\text{mol}^{-1}$. Note that complex **E**, the product of direct H_3SiOMe elimination from **D** containing a terminal $\kappa\text{P}-\text{C}\equiv\text{P}^-$ ligand, is about $\Delta H = 34$ kcal $\cdot\text{mol}^{-1}$ less stable than **F**.^[54]

The cyaphido complex **8** proved to be remarkable inert, and was unable to serve as a precursor to bimetallic complexes containing a bridging cyaphido ligand ($[\text{M}-(\text{C}\equiv\text{P})-\text{M}']$). However, it demonstrated the accessibility of terminal cyaphido complexes by desilylation of silylphosphaalkynes, and served as the first example in a series of cyaphido complexes of the type $[\text{M}(\text{R})(\eta^1-\text{C}\equiv\text{P})(\text{dppe})_2]$ enabled by this synthetic route.

In 2012, Russell and co-workers investigated the coordination chemistry of trimethylsilylphosphaalkyne, $\text{Me}_3\text{Si}-\text{C}\equiv\text{P}$, towards selected transition metal complexes and synthesized, *inter alia*, the bis(phosphaalkyne) complex $[\text{Mo}(\eta^1-\text{P}\equiv\text{C}-\text{SiMe}_3)_2(\text{dppe})_2]$. However, the desilylation protocol reported by Grützmacher and co-workers did not lead to a cyaphido complex. Instead, addition of tetrabutylammonium difluorotriphenylsilicate (TBAT) as a fluoride source showed evidence for the formation of a mixed phosphalkyne-cyaphido complex of the type $[\text{Mo}(\eta^1-\text{P}\equiv\text{C}-\text{SiMe}_3)(\eta^1-\text{C}\equiv\text{P})(\text{dppe})_2]$ (**9**, Figure 8). Two low-field shifted multiplets at $\delta = 197.8$ ppm and $\delta = 183.0$ ppm were observed in the $^{31}\text{P}\{^1\text{H}\}$ NMR spectrum, and resonances consistent with the formation of the expected by-products PH_3SiF and Me_3SiF could be detected in the ^{19}F spectrum. Unfortunately, it was not possible to further characterize compound **9**.^[55]

With the aim to analyze the electronic properties of cyaphido-complexes more closely, Crossley and co-workers

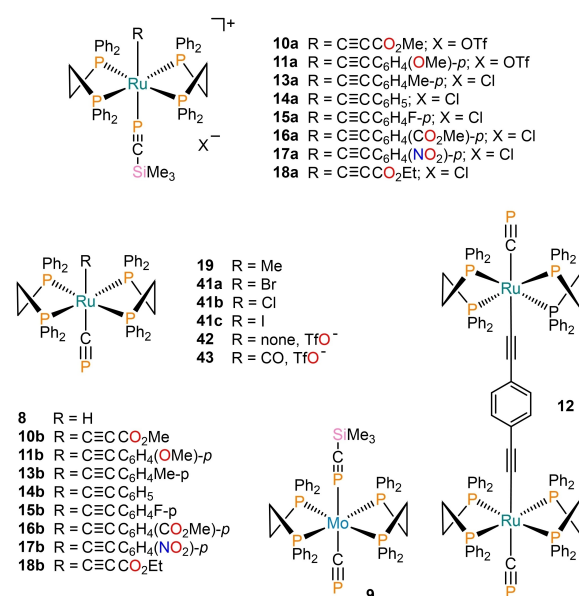


Figure 8. Overview of phosphalkyne coordination compounds $[\text{Ru}(\text{dppe})_2(\eta^1-\text{P}\equiv\text{CSiMe}_3)(\text{C}\equiv\text{CR})][\text{X}]$ and cyaphido complexes of the type $[(\text{dppe})_2\text{M}(\eta^1-\text{C}\equiv\text{P})(\text{L})]$ ($\text{M} = \text{Ru}, \text{Mo}$).

synthesized two new cyaphido ruthenium complexes in 2014, in which the $(\text{C}\equiv\text{P})^-$ ligand was located *trans* to arylacetylide ligands (Figure 8). This coordination geometry was expected to give rise to strong electronic communication between both ligands via the ruthenium(II) center. Two ruthenium acetylide complexes $[\text{Ru}(\text{Cl})(\text{dppe})_2(\text{C}\equiv\text{CR})]$ were first converted *in situ* to the respective triflate salts, followed by addition of $\text{Me}_3\text{Si}-\text{C}\equiv\text{P}$. The resulting complexes, $[\text{Ru}(\text{dppe})_2(\eta^1-\text{P}\equiv\text{C}-\text{SiMe}_3)(\text{C}\equiv\text{CR})][\text{OTf}]$ [$\text{R} = \text{CO}_2\text{Me}$ (**10a**), $p\text{-C}_6\text{H}_4\text{OMe}$ (**11a**)], showed quintet resonances for the cyaphide moiety in their $^{31}\text{P}\{^1\text{H}\}$ NMR spectra [**10a**: $\delta(^{31}\text{P}) = 108.4$ ppm ($^2J_{\text{P-P}} = 35$ Hz); **11a**: $\delta(^{31}\text{P}) = 113.1$ ppm ($^2J_{\text{P-P}} = 34$ Hz)], respectively. Doublets in the $^{13}\text{C}\{^1\text{H}\}$ spectra for the coordinated phosphalkynes were also observed [**10a**: $\delta(^{13}\text{C}) = 192.4$ ppm ($^1J_{\text{P-C}} = 89.9$ Hz); **11a**: $\delta(^{13}\text{C}) = 188.2$ ppm ($^1J_{\text{P-C}} = 88.7$ Hz)].

The crystallographically determined $\text{C}\equiv\text{P}$ distance in **10a** was found to be 1.528(11) Å. By analogy with the $\text{Ph}_3\text{Si}-\text{C}\equiv\text{P}$ complex $[\text{RuH}(\text{dppe})_2(\eta^1-\text{P}\equiv\text{C}-\text{SiPh}_3)][\text{OTf}]$ (see above), treatment of **10a** and **11a** with an alkoxide, such as KO^tBu , resulted in desilylation and rearrangement to give the cyaphido complexes **10b** and **11b**, respectively (Figures 8, 9).

While Grützmacher and co-workers observed an intermediate spectroscopically during the reversible attack of phenolate at the phosphorus atom, Crossley and co-workers could not find any evidence for such a species, even when conducting *in situ* NMR measurements at $T = -78$ °C. It was concluded that the decreased electrophilicity of the phosphorus atom in **10a/11a** combined with the less sterically shielded leaving group favored direct nucleophilic attack at the SiMe_3 moiety. As a result, the reaction time for the generation of the cyaphido complex was significantly shorter. Both coordination compounds **10b** and **11b** show

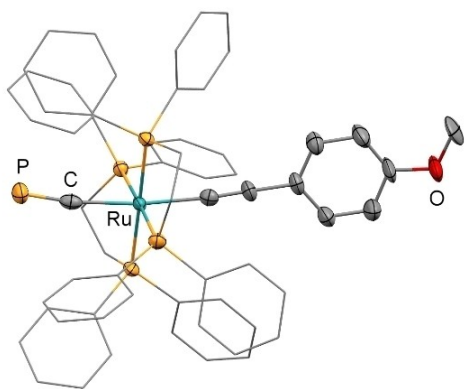


Figure 9. Solid-state molecular structure of **11b**.

substantially high-field shifted NMR resonances [**10b**: $\delta(^{31}\text{P}\{^1\text{H}\}) = 161.5$ ppm (s), $\delta(^{13}\text{C}\{^1\text{H}\}) = 279.1$ ppm (m); **11b**: $\delta(^{31}\text{P}\{^1\text{H}\}) = 159.5$ ppm (m), $\delta(^{13}\text{C}\{^1\text{H}\}) = 281.9$ ppm (m)] compared to the phosphalkyne analogs. The $\text{C}\equiv\text{P}$ stretching frequencies were observed at 1255 cm^{-1} and 1261 cm^{-1} for **10b** and **11b** in their respective IR spectra. This is consistent with slightly stronger $\text{C}\equiv\text{P}$ bonds compared to **8**, due to competition of the cyphido ligand with the *trans*-acetylide ligand for π back donation from the metal center. A single crystal X-ray diffraction study of $[\text{Ru}(\text{dppe})_2(\eta^1\text{-P}\equiv\text{C}-\text{SiMe}_3)(\text{C}\equiv\text{C}-p\text{-C}_6\text{H}_4\text{OMe})][\text{OTf}]$ (**11b**) confirmed the presence of a shorter $\text{C}\equiv\text{P}$ bond length ($1.544(4)$ Å; cf. $1.573(2)$ Å for **8**).

The conjugated π -system slightly deviates from linearity ($\text{Ru}-\text{C}\equiv\text{C}$ $174.4(3)^\circ$; $\text{Ru}-\text{C}\equiv\text{P}$ $172.3(2)^\circ$). Calculations show that in both cases the HOMO and HOMO-1 consist of the out-of-phase mixing of $\text{Ru}(d_{xy}, d_{xz})$, $\text{C}\equiv\text{C}(\pi)$ and $\text{C}\equiv\text{P}(\pi)$ orbitals, with a considerable contribution from the cyphido moiety (**10b**: 50% $\pi(\text{C}\equiv\text{P})$ for both orbitals; **11b**: 24% $\pi(\text{C}\equiv\text{P})$ HOMO, $\pi(\text{C}\equiv\text{P})$ 43% HOMO-1). The HOMO-LUMO gap (ΔE **10b**: 3.5 eV, **11b**: 3.7 eV) of both complexes differs by 0.2 eV. The LUMOs are dominated by the dppe ligands, and the $\text{C}\equiv\text{P}$ π^* orbitals do not contribute perceptibly to anti-bonding orbitals until LUMO+18/19. The lone pair of the cyphido ligand lies about 1.6 eV below the HOMO (**10b**: HOMO-6, **11b**: HOMO-7) and possesses about 75% *s*- and 25% *p*-orbital character. A combined UV/Vis spectroscopy and TD-DFT (TD=time dependent) study allows the assignment of a strong absorption around $\lambda = 250$ nm in both compounds as LLCT (ligand-to-ligand charge transfer) bands in which an electron is excited from the CP/CC π MO to the dppe π^* orbitals. A second band at about $\lambda = 300$ nm was observed for **11b**. Other less pronounced absorptions arise mainly from ILCT (intra-ligand charge transfer) and are assigned to π and π^* transitions.^[56]

In a continuation of their work, in 2018 Crossley and co-workers reported a bimetallic complex bearing two conjugated $\text{C}\equiv\text{P}$ moieties (**12**, Figure 8). The reaction of $[\{\text{Ru}(\text{dppe})_2\}_2\{\mu-(\text{C}\equiv\text{C})_2(\text{C}_6\text{H}_4-p)\}\text{Cl}_2]$ with two equivalents of AgOTf and $\text{Me}_3\text{Si}-\text{C}\equiv\text{P}$ afforded the corresponding linear bis-ethynylbenzene-bridged bimetallic complex with two terminal phosphalkyne groups. This compound showed a

resonance at $\delta(^{31}\text{P}) = 111.4$ ppm ($^3J_{\text{P-P}} = 34$ Hz). Subsequent treatment with KOtBu cleaved the trimethylsilyl groups and gave the new complex **12** with two terminal cyphido ligands. NMR spectroscopy revealed a doublet at $\delta(^{31}\text{P}\{^1\text{H}\}) = 159.7$ ppm ($^3J_{\text{P-P}} = 48.3$ Hz) and $\delta(^{13}\text{C}\{^1\text{H}\}) = 281.8$ ppm ($^1J_{\text{C-P}} = 92.0$ Hz) for the $\text{C}\equiv\text{P}$ moiety. In the IR spectrum of **12**, the $\text{C}\equiv\text{P}$ stretching mode was recorded at $\tilde{\nu} = 1247\text{ cm}^{-1}$. Calculations of the frontier orbitals showed some degree of conjugation. The lone pairs at the phosphorus atoms of the terminal cyphido ligands are strongly stabilized (HOMO-14 and HOMO-15) with about 75% *s*- and 25% *p*-orbital character. The observed and calculated UV/Vis spectra confirmed a dominance of LLCT (both bis-ethynylbenzene bridge and cyphido ligands) as well as MLCT (metal-to-ligand charge transfer) transitions to the dppe scaffold resulting in absorption bands at $\lambda = 370$ and $\lambda = 250$ nm.^[57]

Building on the idea of linking the conjugated π systems of acetylide and cyphido ligands by transition-metal centers, Crossley and co-workers published a series of *trans*-cyphido-acetylide complexes in 2019. Starting from the ruthenium-acetylide precursors *trans*- $[\text{Ru}(\text{dppe})_2(\text{C}\equiv\text{CR})\text{Cl}]$ ($\text{R} = \text{C}_6\text{H}_4\text{Me-}p$ **13a**, C_6H_5 **14a**, $\text{C}_6\text{H}_4\text{F-}p$ **15a**, $\text{C}_6\text{H}_4(\text{CO}_2\text{Me})-p$ **16a**, $\text{C}_6\text{H}_4(\text{NO}_2)-p$ **17a**, CO_2Et **18a**), substitution of the chloride ligand by $\text{Me}_3\text{Si}-\text{C}\equiv\text{P}$ using AgOTf , AgPF_6 or $\text{Tl}(\text{OTf})$ as halide abstracting reagents afforded the corresponding *trans*- $[\text{Ru}(\text{dppe})_2(\eta^1\text{-P}\equiv\text{C}-\text{SiMe}_3)(\text{C}\equiv\text{CR})]^+$ salts, which all exhibited a characteristic resonance at around 110 ppm in their ^{31}P NMR spectra for the η^1 -phosphalkyne ligand. The respective cyphido complexes (**13b-18b**) were obtained by addition of KOtBu . Notably, the purity and yield were affected by the counterion (triflate > hexafluorophosphate salts) and the presence of trace quantities of silver salts, which promoted the formation of unknown side-products. This problem was avoided by using $\text{Tl}(\text{OTf})$ instead, which allowed for facile reactions at room temperature. In accordance with the previously conducted reactions (cf. **10b**, **11b**) no intermediates of the type $[\text{RuH}(\text{dppe})_2\{\text{C}(\text{SiMe}_3)=\text{P}(\text{OtBu})\}]$ could be observed, even at low temperatures ($T = -78^\circ\text{C}$). The NMR and UV/Vis spectroscopic data, as well as a selection of structural information for complexes **15b** and **16b** are depicted in Table 1 and 2. Their evaluation revealed a general trend that correlates with the donor/acceptor properties of the terminal $-\text{C}\equiv\text{C}-\text{R}$ substituent. The ^{31}P chemical shifts of the $\text{C}\equiv\text{P}$ moiety slightly increase with increased electron-withdrawing character of the *trans*-substituent, while the cyphido ^{13}C NMR shifts follow the opposite trend. This behavior is in line with calculations showing extensive out-of-phase mixing of the $\text{Ru}(d_{xy}, d_{xz})$, $\text{C}\equiv\text{C}(\pi)$ and $\text{C}\equiv\text{P}(\pi)$ in the HOMO and HOMO-1 resulting in a certain amount of metal-mediated conjugation. Consequently, these complexes can be considered as analogs of classical *trans*-bis-acetylides, which is in line with the isolobal relationship between a cyphido and an acetylide ligand. In all cases the π^* system of the cyphido ligand contributes significantly only to LUMOs of high energy (> LUMO+17), around 5 eV above the HOMO. Thus, the electronic spectra are mainly designated as LLCT and MLCT transitions from the HOMO/HOMO-1

(mainly $C\equiv C(\pi)$ and $C\equiv P(\pi)$) to the chelating dppe ligands. They reveal an intense band at $\lambda=300$ nm for **13b–15b** and $\lambda=350$ nm for **16b** and **17b**.^[58]

Targeting follow-up reactions at the cyaphido ligand (cf. Section 5), Crossley and co-workers synthesized a modified ruthenium cyaphido complex with the intention of generating an accessible cyaphido moiety. Starting from the literature-known complex $[Ru(dppe)_2Me_2]$,^[59] CH_3^- elimination with $Tl(OTf)$ afforded $[Ru(dppe)_2Me][OTf]$. Subsequent addition of $Me_3Si-C\equiv P$ gave *trans*- $[Ru(dppe)_2(Me)(\eta^1-P\equiv C-SiMe_3)][OTf]$ which exhibited characteristic NMR resonances at $\delta(^{31}P\{^1H\})=121.3$ ppm (q, $^2J_{P-P}=28$ Hz) and $\delta(^{13}C\{^1H\})=185.1$ ppm (d, $^1J_{C-P}=69$ Hz) for the phosphalkyne ligand. Elimination of the trimethylsilyl group with phenolate generated the corresponding neutral cyaphido complex *trans*- $[Ru(dppe)_2(Me)(\eta^1-C\equiv P)]$ (**19**, Figure 8), which showed broad NMR signals at $\delta(^{31}P\{^1H\})=177.9$ ppm and $\delta(^{13}C\{^1H\})=294.3$ ppm for the cyaphido ligand. The molecular structure of **19** in the solid state was confirmed by single crystal X-ray diffraction methods, albeit with some uncertainty regarding the C–P bond length due to minor crystallographic disorder. Nevertheless, the $C\equiv P$ and Ru–C distances as well as the P–C–Ru angle of $165.5(5)^\circ$ are in agreement with other known ruthenium cyaphido complexes.^[60]

3.4. Generation of $(C\equiv P)^-$ from aryl phosphalkynes by oxidative addition of $C(sp)-C(sp^2)$ -bonds to Pt^0

While many cyaphido complexes are still prepared via the desilylation method established by Grützmacher and co-workers, the group of Müller followed an alternative method to generate the cyaphido ligand from η^2 -phosphalkynes in the coordination sphere of a metal center. Nitriles and phosphalkynes are valence isoelectronic species. Moreover, there is a well-known isolobal relationship between substituted acetylenes and phosphalkynes. From a conceptual point of view, this could be used as a strategy to access cyaphido complexes by oxidative addition of phosphalkynes to a metal center. Precedent for this type of reactivity has been reported by Jones and co-workers who established that $C(sp)-C(sp^2)$ bond cleavage in aryl-nitriles is thermally viable using nickel(0) complexes, and in aryl-alkynes is viable photochemically using platinum(0) complexes (Figure 10).^[61,62]

Accordingly, Jones, Müller and co-workers prepared a series of platinum- η^2 -phosphalkyne complexes by reaction of $[Pt(COD)_2]$ (COD=1,5-cyclooctadiene) with an aryl-phosphalkyne and a chelating diphosphine as co-ligand. The corresponding η^2 -phosphalkyne complexes were used as precursors for the generation of the cyaphido compounds, starting with the complex $[(dippe)Pt(\eta^2-P\equiv C-Mes)]$ (dippe = 1,2-bis(diisopropylphosphino)ethane, Mes = mesityl) (**20a**). Indeed, irradiation with UV light ($\lambda=365$ nm) showed a new set of upfield-shifted phosphorus resonances in the $^{31}P\{^1H\}$ NMR spectrum with different coupling constants, particularly for the $C\equiv P$ moiety [$\delta(^{31}P\{^1H\})=97.8$ ppm (dd, $^2J_{Pt-P}=340$ Hz) **20b** vs. 138.3 ppm (dd, $^2J_{Pt-P}=230$ Hz) **20a**], with

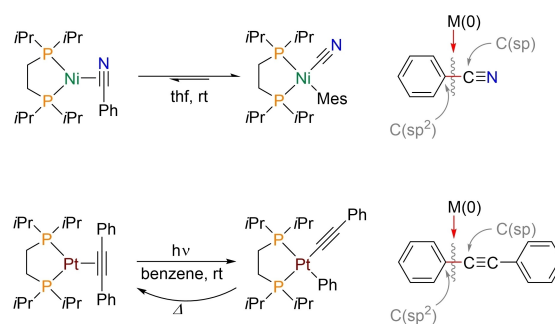
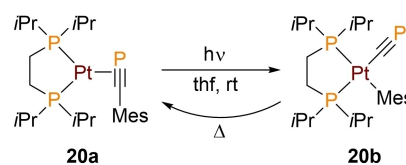


Figure 10. $C(sp)-C(sp^2)$ bond cleavage in benzonitrile and diphenylacetylene.

respect to the starting material. This change indicated the expected C–CP bond cleavage reaction and the formation of a platinum(II) complex (Scheme 5). Even though the photochemical reaction successfully generated the cyaphido complex $[(dippe)Pt(\eta^1-C\equiv P)(Mes)]$ (**20b**), conversion was low due to a concurrent thermal reductive elimination leading to the starting compound **20a** again. Based on the experimental and theoretical work of Weigand and González on the photochemical cleavage of the $C(sp)-C(sp^2)$ bond in Pt^0 diphenylacetylene complexes,^[63–65] the light source ($\lambda_{max}=405$ nm, 4×15 W blacklight LED) was changed to improve the outcome of the photochemical reaction. In combination with the more sterically demanding dcpe (1,2-bis(dicyclohexylphosphino)ethane) ligand, the maximum conversion to the σ -complex **21b** could be increased to as much as 80%.^[66] The Pt^{II} cyaphido complex **21b** could be characterized crystallographically (Figure 11). The cyaphido



Scheme 5. UV light-induced bond activation in $Mes-C\equiv P$ in the coordination sphere of $(dippe)Pt$ and thermal reductive elimination.

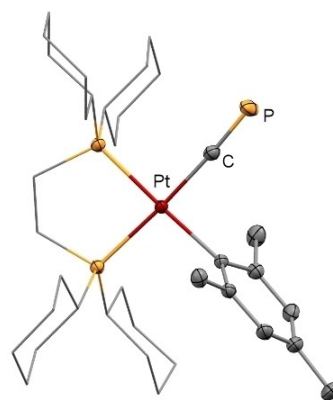


Figure 11. Solid-state molecular structure of **21b**.

ligand showed a resonance at $\delta(^{31}\text{P}\{^1\text{H}\})=96.6$ ppm (dd, $^{2,3}J_{\text{P-P}}=17.7, 10.4$ Hz, $^2J_{\text{P-Pt}}=338$ Hz) and a stretching vibration at $\tilde{\nu}=1259$ cm^{-1} in the corresponding IR spectrum.

Single crystal X-ray diffraction revealed a square planar complex with a $\text{C}\equiv\text{P}$ bond length of 1.5625(18) Å, a Pt–C distance of 2.0920(16) Å and an almost linear Pt–C–P arrangement (176.62(12)°).

Subsequently, modifications at the co-ligand were carried out to favor the oxidative addition process of the η^2 -bound phosphalkyne. Thus, the diphosphine dcpm (bis(dicyclohexylphosphino)methane), with a smaller bite angle than dpe, was selected. It is well established that smaller bite angles generally favor oxidative addition reactions at the metal center.^[67] Interestingly, the phosphalkyne complex [(dcpm)Pt(η^2 -P=C-Tripp)] (Tripp=(2,4,6-triisopropyl)phenyl) (**22a**) indeed transforms upon irradiation to the isolable cyaphido complex [(dcpm)Pt(η^1 -C≡P)-(Tripp)] (**22b**) without any evidence of reversibility or the formation of by-products at room temperature.

Even though the isolated cyaphido complex **22b** is stable at room temperature and at slightly elevated temperatures, computational studies on the reductive elimination process for the simplified model complex [(dmpm)Pt(η^1 -C≡P)(Mes)] (dmpm=bis(dimethylphosphino)methane) revealed the challenges associated with inhibiting the back reaction. The phosphalkyne- π -complex is thermodynamically favored over the cyaphido complex by approximately $\Delta G=-26$ kcal·mol⁻¹ and only suppressed by a modest activation barrier of $\Delta G=29$ kcal·mol⁻¹ (Figure 12). It is therefore not surprising that persistent heating of **22b** still slowly regenerates **22a**. The analysis of the frontier orbitals showed a significant contribution of the (C≡P)⁻ ligand to the LUMO, which is located 8.50 eV above the HOMO (absolute value).

Moreover, a high contribution of the C≡P π -orbitals were assigned to the HOMO–1 and HOMO–3, while the lone pair of the terminal phosphorus atom substantially contributes to the HOMO–6. These observations contrast the calculations performed for the $\text{L}_n\text{Ru}-\text{C}\equiv\text{P}$ systems and may be important for follow-up reactions at the cyaphido ligand (see section 5).^[66] It should be mentioned here that

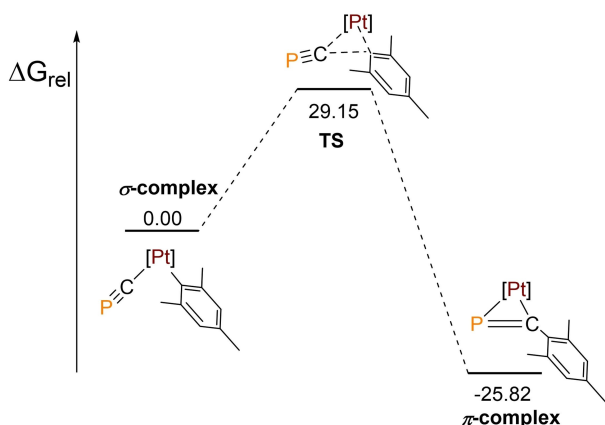


Figure 12. Energy diagram for the thermal reductive elimination reaction in the complex [(dmpm)Pt(η^1 -C≡P)(Mes)].

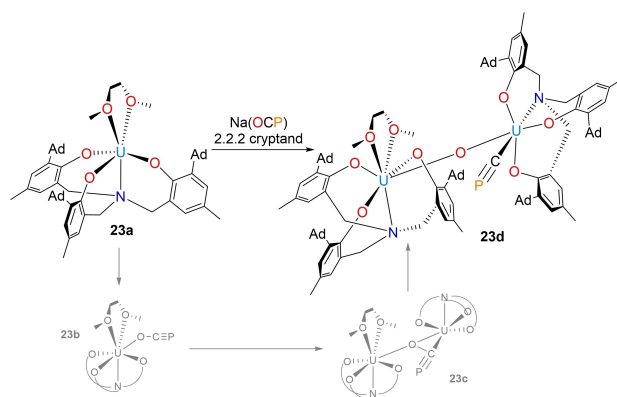
the C–C bond activation in aryl-substituted phosphalkynes is a prime example for the diagonal relationship between carbon and phosphorus in the periodic table of the elements.

3.5. Generation of (C≡P)⁻ by reductive C–O bond cleavage in (OCP)⁻

Developments in the chemistry of the 2-phosphaethynolate ion inspired the prospect of utilizing it to generate the cyaphide ion by reductive C–O bond cleavage.^[3] In 2017, Meyer and co-workers demonstrated this through the synthesis of a diuranium cyaphido complex from Na(O–C≡P). The reaction of Na(O–C≡P) with the U^{III} chelate complex **23a** and the subsequent addition of [2.2.2]Cryptand (4,7,13,16,21,24-hexaoxa-1,10-diazabicyclo-[8.8.8]hexacosane) in DME resulted in the formation of the paramagnetic dinuclear cyaphido complex [Na(2.2.2-crypt)]-[[((^{Ad,Me}ArO)₃N)U(DME)](μ-O){((^{Ad,Me}ArO)₃N–U(η^1 -C≡P))} (^{Ad,Me}ArO)₃N³⁻=trianion of tris(2-hydroxy-3-(1-adamantyl)-5-methylbenzyl)amine) (**23d**, Scheme 6). The phosphorus resonance of the C≡P moiety was found at $\delta(^{31}\text{P}\{^1\text{H}\})=265.8$ ppm. Single crystal X-ray structure determination revealed a short C≡P bond length of 1.523(8) Å and a U–C distance of 2.570(7) Å. The U–C–P angle was found to be nearly linear (177.5(4)°) (Figure 13).

Additional computational studies were performed to determine the oxidative addition mechanism. In a first one-electron transfer step, (O–C≡P)⁻ coordinates to the U^{III} center via the oxygen atom, resulting in the mononuclear U^{IV} intermediate **23b** (Scheme 6). Due to the exceptional oxophilicity and reducing power of U^{III}, a second equivalent of **23a** coordinates to the oxygen atom affording the key intermediate **23c**.

Compound **23c** contains a (O–C≡P)³⁻ entity, which is sandwiched between two U^{IV} centers via $\eta^2, \kappa\text{O}:\kappa\text{C}$ -coordination to one uranium center, and via $\eta^1, \kappa\text{O}$ coordination to the second uranium atom. This enables facile O–C bond



Scheme 6. [Na(2.2.2-crypt)]-[[((^{Ad,Me}ArO)₃N)U^{IV}(DME)](μ-O)-{((^{Ad,Me}ArO)₃N–U^{IV}(η^1 -C≡P))} and proposed pathway. The [Na(2.2.2-crypt)] cation is not depicted.

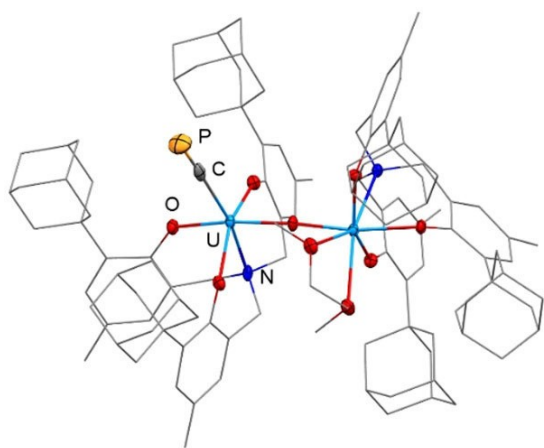


Figure 13. Solid-state molecular structure of **23d**. The [Na(2.2.2-crypt)] cation is omitted for clarity.

cleavage (activation barrier $\Delta H = 4.4 \text{ kcal}\cdot\text{mol}^{-1}$), resulting in **23d**.^[68]

3.6. Generation of $(\text{C}\equiv\text{P})^-$ by reductive C–O bond cleavage in $\text{R}_3\text{SiO}-\text{C}\equiv\text{P}$

Building on the finding that a cyaphido ligand can be generated by reductive C–O bond cleavage of the phosphaethyndiolate anion in the coordination sphere of a strongly oxophilic metal center, Goicoechea and co-workers reasoned that reduction of a functionalized phosphaethyndiolate may offer the possibility of a more facile generation of the cyaphide ion. In 2021, the group succeeded in accessing the Grignard-type reagents **24a–d**, which, for the first time, can be used to transfer the cyaphide ligand to other metal centers using a simple salt-metathesis protocol. (Figure 14, Table 1). *In situ* silylation of $[\text{Na}(\text{dioxane})_x](\text{PCO})$ with $i\text{Pr}_3\text{SiOTf}$ resulted in the formation of the literature-known kinetic product $i\text{Pr}_3\text{SiO}-\text{C}\equiv\text{P}$.^[69] Subsequent reduction with Jones' magnesium(I) reagent^[70] $[\text{Mg}(\text{DippNaCNac})]_2$ ($\text{DippNaCNac} = N,N'$ -bis(2,6-diisopropylphenyl)pentane-2,4-diimine) afforded an equimolar mixture of the cyaphido Grignard reagent $[\text{Mg}(\text{DippNaCNac})(\eta^1-\text{C}\equiv\text{P})(\text{dioxane})]$ (**24a**) and the by-product $\text{Mg}(\text{DippNaCNac})(\text{OSi}i\text{Pr}_3)(\text{dioxane})$ (**25**).

Computational studies suggested an exergonic mechanism ($\Delta G = 52.2 \text{ kcal}\cdot\text{mol}^{-1}$) with a moderate energy barrier of $\Delta G = 12.5 \text{ kcal}\cdot\text{mol}^{-1}$ (Scheme 7).

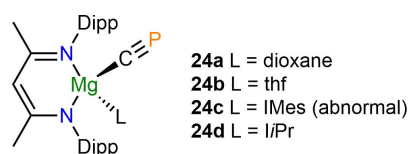
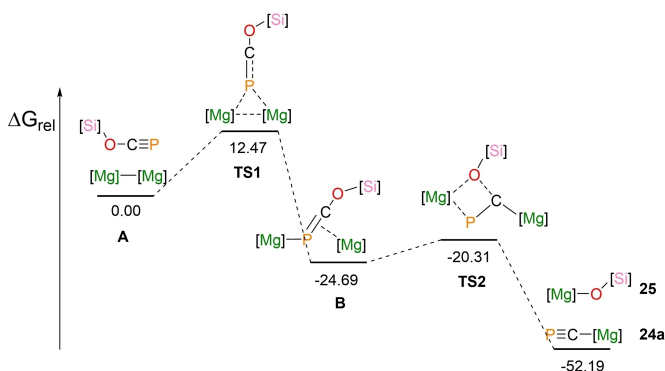


Figure 14. Cyaphide transfer reagents **24a–d**.



Scheme 7. Mechanism for the formation of **24a**; ΔG in $\text{kcal}\cdot\text{mol}^{-1}$.

Initially, the $i\text{Pr}_3\text{SiO}-\text{C}\equiv\text{P}$ symmetrically approaches the dimagnesium core of Jones' reagent via the phosphorus atom, before forming a metalla-phosphaalkene intermediate. This species subsequently initiates the Mg–Mg bond cleavage, which finally leads to a stabilized intermediate (structural evidence for a comparable intermediate has also been recently reported).^[71]

The terminal and side-on bound $\text{P}=\text{C}-\text{O}$ entity goes through a transition state consisting of a four-membered ring (Scheme 7, TS2), favored by the strong oxophilicity of magnesium. This leads to the cleavage of the C–O bond of the phosphaethyndiolate moiety and formation of two independent Mg^{II} monomers. Substantial steric protection is essential, as the slightly less sterically shielded $[\text{Mg}(\text{MesNaCNac})]_2$ ($\text{MesNaCNac} = N,N$ -bis(2,4,6-trimethylphenyl)pentane-2,4-diimine) compound produces a reaction mixture containing cyaphide-based oligomers. In the NMR spectrum, the phosphorus resonance for the $\text{C}\equiv\text{P}$ moiety of $[\text{Mg}(\text{DippNaCNac})(\eta^1-\text{C}\equiv\text{P})(\text{dioxane})]$ was found at $\delta(^{31}\text{P}\{-^1\text{H}\}) = 177.2 \text{ ppm}$, and the cyaphido carbon NMR shift was observed at $\delta(^{13}\text{C}\{^1\text{H}\}) = 271.0 \text{ ppm}$ (d, $^1J_{\text{C-P}} = 34 \text{ Hz}$). The crystallographic characterization of **24a** revealed a tetrahedral structure with a linear arrangement of the $\text{Mg}-\text{C}\equiv\text{P}$ moiety ($177.37(15)^\circ$) (Figure 15). The molecular structure of **24a** also showed typical distances of $2.118(2) \text{ \AA}$ and $1.553(2) \text{ \AA}$ for the Mg–C and $\text{C}\equiv\text{P}$ bond, respectively. Due to an overlap with ligand-centered aromatic stretching modes, the $\text{C}\equiv\text{P}$ stretching vibration ($\tilde{\nu} = 1347 \text{ cm}^{-1}$) was determined by means of theoretical calculations. The similar solubility of

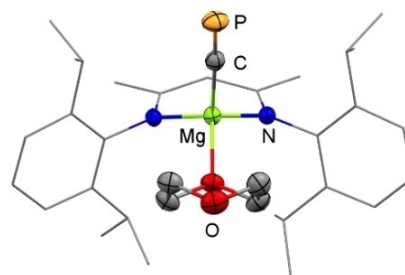


Figure 15. Solid-state molecular structure of **24a**.

24a and **25** allowed the isolation of **24a** in only very low yields, which was further exacerbated by its instability under vacuum. The use of dioxane-free $\text{Na}(\text{O}-\text{C}\equiv\text{P})$ in the reaction resulted in low conversion due to its poor solubility in non-coordinating solvents, although it affords a solvent-free analog of **24a** with a yet unknown composition and a singlet resonance in the NMR spectrum at $\delta(^{31}\text{P}\{^1\text{H}\})=246.7$ ppm (this is believed to be a cyclic trimer as observed for $[\text{Mg}(\text{MesNacNac})(\text{C}\equiv\text{N})_3]$).^[72] However, due to rapid decomposition, the isolation of this species was unsuccessful.

Addition of the *N*-heterocyclic carbenes (NHCs) IMes or IiPr (IMes = 1,3-bis(2,4,6-trimethylphenyl)imidazol-2-ylidene; IiPr = 1,3-diisopropyl-imidazol-2-ylidene) to a crude mixture of **24a** and **25** successfully displaced the coordinated dioxane and afforded the stable carbene adducts $[\text{Mg}(\text{DippNacNac})(\eta^1-\text{C}\equiv\text{P})(\text{IMes})]$ (**24c**) and $[\text{Mg}(\text{DippNacNac})(\eta^1-\text{C}\equiv\text{P})(\text{IiPr})]$ (**24d**), which could be isolated as stable compounds in the solid state (Figure 14). Both compounds showed similar chemical shifts in their NMR spectra [$\delta(^{31}\text{P}\{^1\text{H}\})=162.9$ ppm (**24c**), 174.9 ppm (**24d**)] and their molecular structures were unambiguously verified by means of single crystal X-ray diffraction. While the IiPr carbene coordinates via a normal NHC coordination mode, the IMes carbene showed “abnormal” coordination in the solid state. The infrared $\text{C}\equiv\text{P}$ stretching vibrations for both compounds were in good agreement with calculated values [**24c**: $\tilde{\nu}=1316$ cm^{-1} (calc.: $\tilde{\nu}=1311$ cm^{-1}), **24d**: $\tilde{\nu}=1325$ cm^{-1} (calc.: $\tilde{\nu}=1325$ cm^{-1})] and supports the accuracy of the calculated value for **24a**.^[73]

4. Transfer of the $(\text{C}\equiv\text{P})^-$ ligand

As described in section 3.6, Goicoechea and co-workers recently reported on the synthesis of $[\text{Mg}(\text{DippNacNac})(\eta^1-\text{C}\equiv\text{P})(\text{dioxane})]$ (**24a**). The highly polar $\text{Mg}-\text{C}\equiv\text{P}$ bond in this complex offers the possibility of performing salt metathesis reactions with metal halides, allowing for transfer of the cyaphido ligand from one metal to another. This possibility was first investigated by reacting **24a** with chlorotrimethylsilane. Indeed, quantitative $(\text{C}\equiv\text{P})^-$ transfer took place, resulting in the formation of the known phosphalkyne $\text{Me}_3\text{Si}-\text{C}\equiv\text{P}$. A similar reaction was observed for the NHC adducts **24c** and **24d**. Next, this metathesis reaction was also successfully demonstrated for the main-group metal compound $[\text{Ge}(\text{DippNacNac})\text{Cl}]$. However, in this case the product $[\text{Ge}(\text{DippNacNac})(\eta^1-\text{C}\equiv\text{P})]$ (**26**) exhibited a tendency to decompose and could not be isolated (Figure 16).

In contrast, the reaction of **24a** with the tin(II) analog afforded $[\text{Sn}(\text{DippNacNac})(\eta^1-\text{C}\equiv\text{P})]$ (**27**), a more stable compound that could be isolated by fractional crystallization. Spectroscopic investigation revealed a phosphorus resonance at $\delta(^{31}\text{P}\{^1\text{H}\})=122.4$ ppm ($^2J_{\text{P-Sn}}=69.8$ Hz). No ^{13}C signal could be found for the cyaphido group, presumably because of broadening due to coupling to the $^{117/119}\text{Sn}$ nuclei. The infrared spectrum revealed a $\text{C}\equiv\text{P}$ stretching mode in accordance with computational calculations ($\tilde{\nu}=1327$ cm^{-1}) at $\tilde{\nu}=1321$ cm^{-1} .

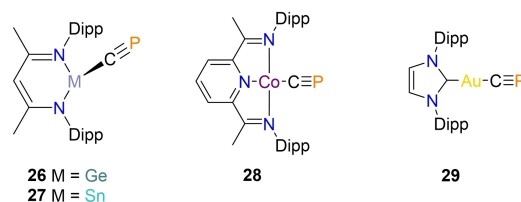


Figure 16. Formation of cyaphido complexes **26–29** by $(\text{C}\equiv\text{P})^-$ transfer via $[\text{Mg}(\text{DippNacNac})(\eta^1-\text{C}\equiv\text{P})(\text{dioxane})]$.

Single crystal X-ray diffraction analysis of **27** revealed a comparable $\text{C}-\text{P}$ distance of 1.542(4) Å with respect to compounds **24a–d** (Figures 14, 17). The $\text{Sn}-\text{C}\equiv\text{P}$ moiety is linear (179.16°) and the $\text{Sn}-\text{C}$ bond is, as expected, rather long (2.216(4) Å).

Next, this cyaphide transfer protocol was successfully applied towards two transition metal complexes, $[(\text{DippPDI})\text{CoCl}]$ ($\text{DippPDI}=1,1'$ -(pyridine-2,6-diyl)bis(*N*-(2,6-diisopropylphenyl)ethan-1-imine)) and $[\text{Au}(\text{IDipp})\text{Cl}]$ ($\text{IDipp}=1,3$ -bis(diisopropylphenyl)-imidazol-2-ylidene). The resulting cobalt(I) complex $[(\text{DippPDI})\text{Co}(\eta^1-\text{C}\equiv\text{P})]$ (**28**) is the first example of a *3d* metal cyaphido complex. The $\text{C}\equiv\text{P}^-$ ligand showed a single resonance in the phosphorus NMR spectrum at $\delta(^{31}\text{P}\{^1\text{H}\})=345.4$ ppm, and a stretching vibration at $\tilde{\nu}=1306$ cm^{-1} in the IR spectrum. Moreover, the molecular structure of the product was unambiguously confirmed by means of X-ray diffraction methods (Figure 18).

The gold(I) complex $[\text{Au}(\text{IDipp})(\eta^1-\text{C}\equiv\text{P})]$ (**29**) showed a singlet resonance in its phosphorus spectrum at $\delta(^{31}\text{P}\{^1\text{H}\})=84.1$ ppm. The carbon signal for the $(\text{C}\equiv\text{P})^-$ ligand was

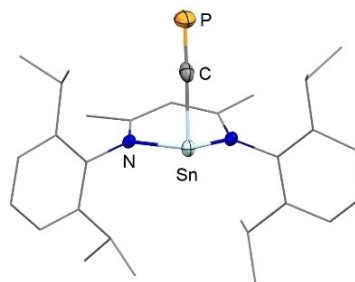


Figure 17. Solid-state molecular structure of **27**.

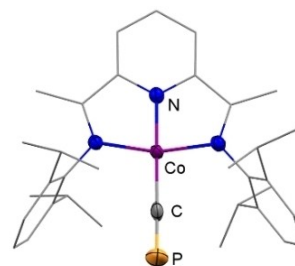


Figure 18. Solid-state molecular structure of **28**.

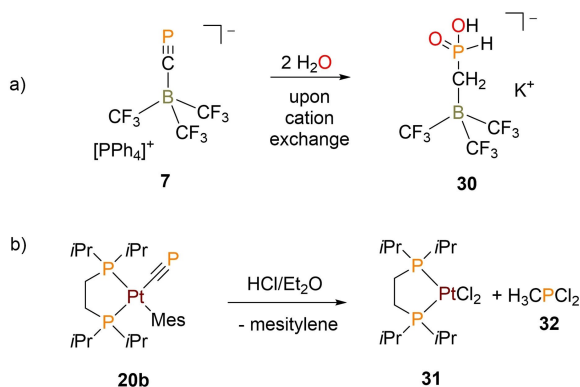
observed at $\delta(^{13}\text{C}\{^1\text{H}\})=247.7$ ppm ($^1J_{\text{C-P}}=6.1$ Hz). The high $\text{C}\equiv\text{P}$ vibrational stretching frequency of $\tilde{\nu}=1342$ cm^{-1} in its infrared spectrum is clearly influenced by coupling to the *trans*-Au–C_{carbene} stretching mode, induced by the linearity of the gold center ($\text{C–Au–C}=178.2(2)^\circ$, $\text{Au–C–P}=178.0(5)^\circ$). The $\text{C}\equiv\text{P}$ bond length of 1.552(6) Å is within the usual range for cyaphido complexes, and an Au–C $\equiv\text{P}$ distance of 1.972(6) Å was found. Interestingly, the Au–C_{carbene} distance of 2.034(6) Å is elongated in comparison to [(IDipp)AuCl] (1.942(3) Å) and is more in line with [Au(IDipp)(η^1 -C $\equiv\text{CPh}$)] (2.018(7) Å), and [Au(IDipp)(η^1 -C $\equiv\text{N}$)] (1.985(15) Å), respectively.^[74] This indicates a similar σ -donor ability of $(\text{C}\equiv\text{P})^-$ compared to $(\text{C}\equiv\text{CPh})^-$ and $(\text{C}\equiv\text{N})^-$, and hints at higher π -accepting ability, corroborating the previous findings of Crossley and co-workers. This seemingly simplistic cyaphido transfer reactivity marks a revolutionary step in the synthetic history of cyaphido compounds. Its utility has already been demonstrated, enabling access to the very first main group metal and 3*d* transition metal cyaphido complexes, as well as the first examples of structurally authenticated metal cyaphido complexes with trigonal pyramidal, square planar, and linear coordination geometries.^[73]

5. Reactivity of the $(\text{C}\equiv\text{P})^-$ ligand

5.1. Reaction with water and hydrogen chloride

Since the preparation of the first cyaphido complexes and cyaphido borates, many attempts have been made to functionalize the $\text{C}\equiv\text{P}$ moiety. The cyaphido borate salt **7** is stable for days in wet acetonitrile solution. However, the attempted cation exchange with $\text{K}[\text{BPh}_4]$ in the presence of moisture led to the formation of $\text{K}[(\text{CF}_3)_3\text{BCH}_2\text{P}(\text{O})(\text{OH})\text{H}]$ (**30**) instead (Scheme 8a).^[50]

Treatment of the Pt^{II} -cyaphido complex **20b** with $\text{HCl}/\text{Et}_2\text{O}$ affords the PtCl_2 complex **31**, mesitylene and H_3CPCl_2 (**32**) (Scheme 8b). While **31** was characterized crystallographically, the formation of **32** was confirmed by means of NMR spectroscopy as well as mass spectrometry.^[75] Presumably, **20b** reacts first with two equivalents of HCl in a



Scheme 8. Reactivity of **7** towards water and reaction of **20b** with $\text{HCl}/\text{Et}_2\text{O}$.

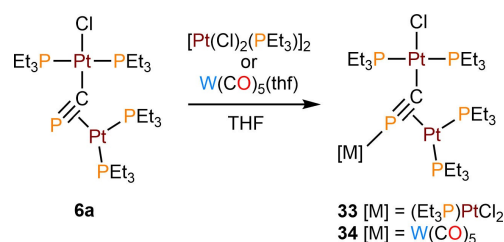
stepwise manner to give $[(\text{dippe})(\text{Mes})\text{Pt–CH}_2\text{PCl}_2]$. The third equivalent of HCl liberates H_3CPCl_2 (**32**) and $[(\text{dippe})\text{Pt}(\text{Cl})(\text{Mes})]$, which reacts with another equivalent of HCl to **31** and mesitylene. This is in line with the observation made by Gier, that treatment of $\text{H–C}\equiv\text{P}$ with excess anhydrous HCl at $T=-110$ °C gives H_3CPCl_2 as the sole product.^[21]

5.2. Reaction with additional transition metal complexes

Similar to other compounds featuring $\text{C}\equiv\text{P}$ triple bonds, e.g. phosphalkynes, the reactivity of the cyaphido ligand is expected to be dominated by its π -system. Investigations on coordination compounds containing η^2 -coordinated phosphalkynes showed that the metal fragment can facilitate the coordination ability of the phosphorus lone pair.^[76] As mentioned above, calculations have shown that the lone pair of the phosphorus atom in cyaphido complexes is energetically stabilized with respect to the π -system, which would prevent an additional coordination via the phosphorus atom. In 1999, the group of Angelici demonstrated the possibility of reacting the cyaphido ligand in **5a** with a second, coordinatively unsaturated transition metal complex. In $[(\text{Cl})(\text{PEt}_3)_2\text{Pt}(\mu\text{-}\eta^1\text{-}\eta^2\text{-C}\equiv\text{P})\text{Pt}(\text{PEt}_3)_2]$ (**6a**) the $\text{C}\equiv\text{P}$ triple bond is sterically blocked for a third coordination on the opposite site of the $\text{C}\equiv\text{P}$ triple bond. Interestingly, addition of either $[\text{Pt}(\text{Cl})_2(\text{PEt}_3)_2]$ or $\text{W}(\text{CO})_5(\text{THF})$ to **6a** afforded the first examples of trinuclear cyaphido complexes with a $\mu_3\text{-}\eta^1\text{-}\eta^2\text{-}\eta^3$ coordination mode [formally $\mu_3\text{-}(\text{M}')\eta^2\text{-}(\text{C}\equiv\text{P})\text{-}(\text{M})\kappa\text{C}\text{-}(\text{M}'')\kappa\text{P}$] $[(\text{Cl}(\text{Et}_3\text{P})_2\text{Pt})\{\mu_3\text{-}\eta^1\text{-}\eta^2\text{-}\eta^3\text{-C}\equiv\text{P}\}\{\text{Pt}(\text{PEt}_3)_2\}_2]$ (**33**) and $[(\text{Cl}(\text{Et}_3\text{P})_2\text{Pt})\{\mu_3\text{-}\eta^1\text{-}\eta^2\text{-}\eta^3\text{-C}\equiv\text{P}\}\{\text{Pt}(\text{PEt}_3)_2\}\{\text{W}(\text{CO})_5\}]$ (**34**), respectively (Scheme 9). While **30** could not be isolated due to its propensity to decompose under vacuum, compound **34** was characterized crystallographically (Figure 19).

The phosphorus atom of the $\text{C}\equiv\text{P}$ moiety in **33** ($\delta(^{31}\text{P}\{^1\text{H}\})=111.2$ ppm) only showed a minor downfield shift of 4 ppm with respect to **6a** ($\delta(^{31}\text{P}\{^1\text{H}\})=107.0$ ppm) in its phosphorus NMR spectrum, whereas the resonance in **34** ($\delta(^{31}\text{P}\{^1\text{H}\})=41.4$ ppm) is strongly upfield shifted by 66 ppm. The molecular structure of **34** in the crystal reveals distorted square-planar coordination environments for both the platinum centers (Figure 19).

The C–P bond length of 1.663(9) Å is identical to that of **6a**, and in line with typical C=P double-bond lengths.^[77] The bent geometry of the $\text{Pt–C}\equiv\text{P}$ moiety (Pt–C–P angle 145.2-



Scheme 9. Reaction of **6a** with additional transition metal complexes.

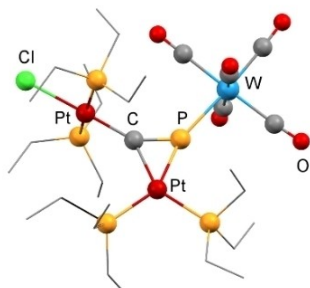


Figure 19. Solid-state molecular structure of **34**.

(6)°, W–P–C 136.1(3)°) indicates a formal sp^2 hybridization of both the phosphorus and the carbon atom, which is consistent with a platinum(II)-character of the metal center.

The dearth of other examples of multimetallic cyaphido complexes reflects a lack of sufficiently reactive terminal cyaphido complexes to serve as precursors. Recently, Yang and Goicoechea found that the reactive linear gold(I) complex [Au(IDipp)(η^1 -C≡P)] (**29**, Figure 16), could react further to form hetero- bi- and tri-metallic cyaphido complexes.^[78] As a matter of fact, while the gold(I) cyanido complex Au(IDipp)(η^1 -C≡N) readily reacts with B(C₆F₅)₃ to afford the $\eta^1:\eta^1$ bridged complex Au(IDipp)(μ_2 -C≡N)B(C₆F₅)₃, the analogous complex [Au(IDipp)(η^1 -C≡P)] (**29**) did not react controllably with commonly used electrophiles, such as [Mo(depe)₂(N₂)₂], [W(CO)₅(THF)], and B(C₆F₅)₃ (depe = 1,2-bis(diethylphosphino)ethane). On the other hand, the reaction of [Au(IDipp)(η^1 -C≡P)] with metal based nucleophiles, such as [Ni(^{Me}iPr)₂(COD)_x] (^{Me}iPr = 1,3-bis(diisopropylphenyl)-4,5-dimethylimidazol-2-ylidene) and [Rh(Cp*)(PMe₃)₂] yields heterobimetallic complexes (Figure 20).

The bimetallic gold(I)-nickel(II) complex [Au(IDipp)(μ - $\eta^1:\eta^2$ -C≡P)Ni(^{Me}iPr)₂] (**35**) shows resonances corresponding to the μ_2 -cyaphido ligand in its phosphorus NMR spectrum at $\delta(^{31}\text{P}\{^1\text{H}\}) = 246.0$ ppm and in its carbon NMR spectrum at $\delta(^{13}\text{C}\{^1\text{H}\}) = 280.3$ ppm (¹J_{C-P} = 105 Hz), and shows a low C≡P stretching frequency of $\tilde{\nu} = 1125$ cm⁻¹ in its Raman spectrum. For the bimetallic gold(I)-rhodium(I) complex [Au(IDipp)(μ - $\eta^1:\eta^2$ -C≡P)Rh(Cp*)(PMe₃)] (**36**), the bridging cyaphido carbon appears in its phosphorus NMR spectrum at $\delta(^{31}\text{P}\{^1\text{H}\}) = 94.7$ ppm (¹J_{P-Rh} = 34 Hz, ²J_{P-P} = 5 Hz), and shows a C≡P stretch mode at $\tilde{\nu} = 1175$ cm⁻¹. The solid state structures of **35** and **36** show that in both cases the cyaphido ligand coordinates to two distinct metal centers in a $\eta^1:\eta^2$ coordination mode (Figure 21)

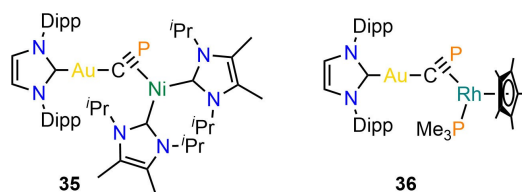


Figure 20. Heterobimetallic complexes **35** and **36**.

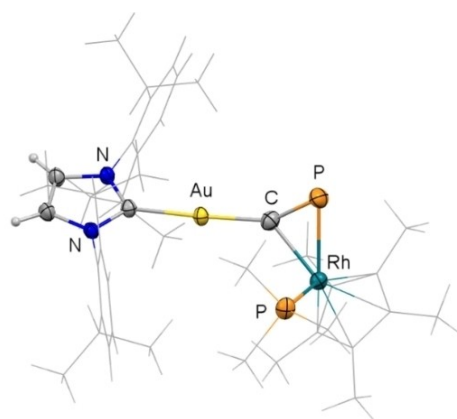


Figure 21. Solid-state molecular structure of **36**.

For **35**, a C≡P bond length of 1.642(4) Å and a Au–C–P bond angle of 146.3(2)° was found, while **36** has a C≡P bond length of 1.631(4) Å and a Au–C–P bond angle of 151.4(3)°. EDA-NOCV analysis correlated with experimentally determined solid-state bond metrics, Raman vibrational spectroscopy, and NMR data confirmed that the η^2 -cyaphido ligand acts as a σ -donor and strong π -acceptor (see Section 2.2). Corroborating the earlier report by Angelici, it is only on blocking the cyaphido π -manifold of **29** in the bimetallic complex **36** that the phosphorus-based lone pair becomes available for further reactivity with electrophiles, allowing access to the heterotrimetallic complex [(Au(IDipp))(μ_3 - $\eta^1:\eta^1$ -C≡P){Rh(Cp*)(PMe₃)}{W(CO)₅}] (**37**).

The μ_3 -cyaphido ligand appears in its phosphorus NMR spectrum as a doublet of doublets with ¹⁸³W satellites at $\delta(^{31}\text{P}\{^1\text{H}\}) = 48.5$ ppm (¹J_{P-W} = 175 Hz, ¹J_{P-Rh} = 62 Hz, ²J_{P-P} = 13 Hz), and shows a Raman stretching frequency of $\tilde{\nu} = 1186$ cm⁻¹. Complex **37** was characterized by single crystal X-ray diffraction, revealing a μ_3 - $\eta^1:\eta^2$ - η^1 -coordination mode (Figure 22), with a C≡P bond length of 1.605(4) Å, a Au–C–P bond angle of 155.4(3)°, and C–P–W bond angle of 144.57(16)°.^[78]

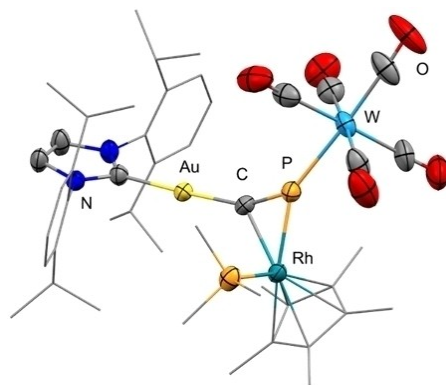


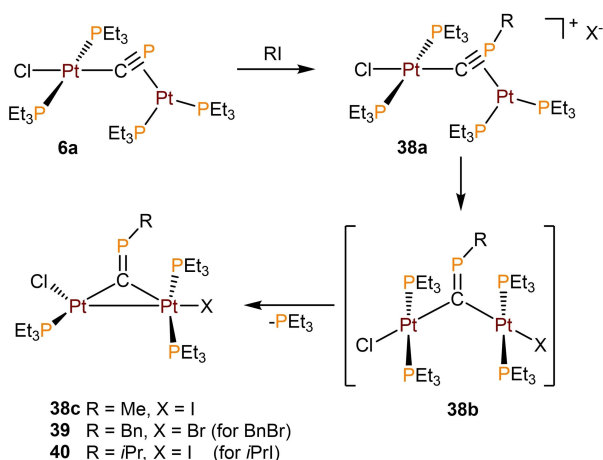
Figure 22. Solid-state molecular structure of **37**.

5.3. Reaction with alkyl halide electrophiles

The functionalization of the cyaphido ligand by organic electrophiles to afford isocyaphide ligands was first investigated by Angelici and co-workers in 1999. The reaction of the μ_2 -cyaphido complex **6a** with excess MeI yielded the methyl isocyaphido complex (Cl)(Et₃P)Pt(μ -C=PMe)Pt(PEt₃)₂(I) (**38c**) (Scheme 10). In this case, MeI methylates the phosphorus atom of the cyaphido ligand resulting in the formation of an isocyaphide (C \equiv P–R) ligand. The reaction also results in the substitution of one of the PEt₃ co-ligands by iodide. This type of reaction is well known for terminal cyanido complexes.^[79] Analogous reactions were attempted for a series of alkyl and aryl halide electrophiles, however only benzyl bromide and isopropyl iodide resulted in the formation of isocyaphide complexes **39** and **40**, respectively. The NMR spectroscopic data showed increased chemical shifts in going from methyl, benzyl to isopropyl ($\delta(^{31}\text{P}\{^1\text{H}\}) = 155.4$ ppm (**38c**), 172.1 ppm (**39**), 200.3 ppm (**40**). The proposed mechanism for the formation of **38c** starts with the initial methylation of the phosphorus atom of the (C \equiv P)[–] ligand, forming the cationic isocyaphide intermediate **38a** (X = I[–], Scheme 10). The subsequent attack of the iodide on the side-on coordinated platinum fragment afforded the bridging isocyaphide intermediate **38b**. This unobserved intermediate then undergoes a rearrangement, forming a Pt–Pt bond with the loss of one PEt₃ ligand, yielding the final product **38c**, which contains a bridging isocyaphide ligand. The cationic complexes **38a'** (not shown) could be isolated and characterized spectroscopically either as a (BPh₄)[–] or (OTf)[–] salt by subsequent addition of NaBPh₄ or MeOTf to **38a** and show a signal in the phosphorus NMR spectrum at $\delta(^{31}\text{P}\{^1\text{H}\}) = 34.7$ ppm.^[79]

5.4. Reactions at the metal center

A further effort to engage the cyaphido ligand in coordination chemistry was undertaken by Crossley and co-workers in 2019. In an attempt to coordinate [ZnBr₂(PPh₃)₂] to the



Scheme 10. Proposed mechanism for the alkylation of **6a**.

phosphorus atom of the cyaphido ligand in *trans*-[Ru(dppe)₂(Me)(η^1 -C \equiv P)] (**19**, Figure 8) both compounds were reacted in a 1:1 ratio. Surprisingly, an unexpected substitution of CH₃[–] for Br[–] occurred, yielding *trans*-[Ru(dppe)₂(Br)(η^1 -C \equiv P)] (**41a**), which was characterized by means of single crystal X-ray diffraction. Bond angles and bond lengths are similar to those observed for **19** and are typical for *trans*-[Ru(dppe)₂(alkyl)(η^1 -C \equiv P)] complexes. The only notable exception is the Ru–CP bond length, which is fairly shortened by around 0.150 Å, reflecting the difference in the *trans*-influence between the weak-field bromido ligand and the strong-field methanido ligand. Further investigations revealed the use of ZnBr₂ in combination with 5 mol-% PPh₃ were the optimal reaction conditions. Applying ZnCl₂ or ZnI₂ resulted in the formation of the analogous halide compounds **41b** and **41c**. The NMR spectroscopic data showed significant shifts for the (C \equiv P)[–] ligand in the halido complex **41a** compared to the methyl precursor **19**. While the phosphorus resonance was shifted upfield by $\Delta\delta(^{31}\text{P}\{^1\text{H}\}) = 46$ ppm, a downfield shift of $\Delta\delta(^{13}\text{C}\{^1\text{H}\}) = 28$ ppm was observed for the carbon NMR signal of the (C \equiv P)[–] carbon atom. The mechanism of the zinc halide-mediated halogen/methyl exchange at a transition metal center still remains unclear. Importantly, halido complexes of this type are inaccessible by conventional routes, because [Ru(dppe)₂(Cl)]⁺ does not react with P \equiv C–SiMe₃. These halide cyaphido complexes are well-suited for metathesis reactions. Indeed, treating **41a** with MgMe₂ resulted in the slow formation of the original complex **19**. The analogous reaction with LiC \equiv CPh only occurred in the presence of Tl(OTf), yielding the *trans*-phenylethynyl cyaphido complex **14b**, which showed a phosphorus signal for the cyaphido ligand, that is shifted upfield by $\Delta\delta(^{31}\text{P}\{^1\text{H}\}) = 16$ ppm compared to **19**. The necessary use of Tl(OTf) as a halide abstracting reagent suggests that the reaction may proceed via the discrete 5-coordinate intermediate [Ru(dppe)₂(η^1 -C \equiv P)](OTf) (**42**). This compound was isolated by addition of Tl(OTf) to **41a**. Compound **42** showed phosphorus resonances in the NMR spectrum at $\delta(^{31}\text{P}\{^1\text{H}\}) = 154$ ppm (q, ³J_{P,P} = 7 Hz) for the cyaphido ligand as well as at $\delta(^{31}\text{P}\{^1\text{H}\}) = 52.1$ ppm (d, ³J_{P,P} = 7 Hz) for the dppe co-ligand. The same reaction was achieved by adding Ag(PF₆) to **41a**, resulting in the analogous PF₆[–] salt. The solid-state structure of **42** revealed a square-pyramidal arrangement around a 5-coordinate ruthenium center (Figure 23). The vacant coordination site in **42** is accessible for further substrates, as demonstrated for a carbonyl ligand by simply passing CO gas through a solution of **42** in dichloromethane.}}

The product [Ru(dppe)₂(CO)(η^1 -C \equiv P)](OTf) (**43**) was characterized crystallographically (C \equiv P distance of 1.53(2) Å), as well as by NMR and IR spectroscopy. The cyaphido ligand in **43** shows a resonance at $\delta(^{31}\text{P}\{^1\text{H}\}) = 181$ ppm in NMR spectrum (q, ³J_{P,P} = 10 Hz), while the C \equiv P stretching vibration was detected at $\tilde{\nu} = 1261$ cm^{–1}. A comparison with the acetylido analog *trans*-[Ru(dppe)₂(CO)(C \equiv CR)]^[59] indicated that the (C \equiv P)[–] ligand acts as an alkynyl analog with slightly enhanced acceptor properties.^[60]}

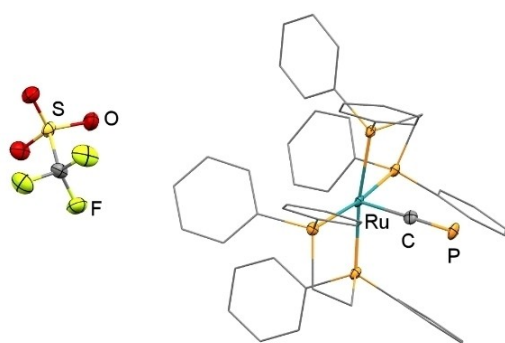
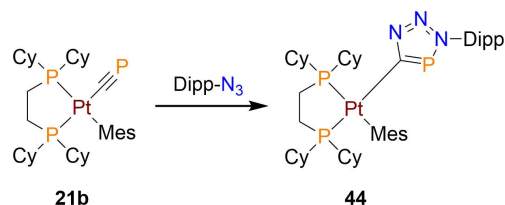


Figure 23. Solid-state molecular structure of **42**.

5.5. [3+2] cycloaddition reactions

[3+2] cycloadditions of phosphalkynes and organic azides are well known.^[80] By analogy to these reactions, Müller and co-workers recently reacted [(dcpe)Pt(η^1 -C≡P)(Mes)] (**21b**) with Dipp-N₃ leading to a regioselective and quantitative [3+2] cycloaddition reaction at room temperature (Scheme 11).

The generation of the triazaphospholato complex **44** was validated by means of NMR spectroscopy and single crystal X-ray diffraction (Figure 24). The phosphorus signal of the 5-membered heterocycle was detected at $\delta(^{31}\text{P}\{\text{H}\}) = 210.9$ ppm (dd, $^2J_{\text{Pt-P}} = 510$ Hz), which is significantly shifted downfield compared to the starting material ($\delta(^{31}\text{P}\{\text{H}\}) = 96.6$ ppm, (dd, $^2,3J_{\text{P-P}} = 17.7, 10.4$ Hz, $^2J_{\text{P-Pt}} = 338$ Hz). Even though **40** is the first reported complex containing an anionic triazaphospholato ligand, the X-ray analysis does not show



Scheme 11. Reaction of **21b** with an organic azide.

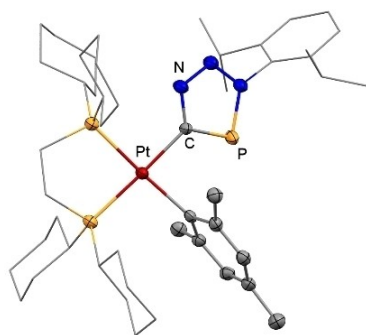


Figure 24. Solid-state molecular structure of **44**.

significant differences in bond lengths and angles compared to neutral 3,5-disubstituted 3*H*-1,2,3,4-triazaphosphole derivatives.^[81] However, this regioselective [3+2] cycloaddition reaction nicely illustrates the possibility of further reactivity at the cyaphido moiety.^[66]

6. Selected NMR- IR- and Crystallographic Data

See Tables 1 and 2.

7. Outlook

The ground-breaking isolation of the first cyaphido metal complex in 1991 demonstrated that this rare pseudo-halide could be used as a ligand in coordination chemistry. Similarly, the discovery and crystallographic characterization of the first transition metal complex with a terminal cyaphido ligand, [*trans*-RuH(η^1 -C≡P)(dppe)₂], hinted at the

Table 1: Selected NMR spectroscopic shifts and IR data.

compound	core metal	$\delta^{31}\text{P}_{(\text{C}\equiv\text{P})}$ [ppm]	$\delta^{13}\text{C}_{(\text{C}\equiv\text{P})}$ [ppm]	$\tilde{\nu}_{(\text{C}\equiv\text{P})}$ [cm ⁻¹]
4a	Pt	68.0	–	–
6a	Pt	107.0	–	–
7	B	39.6	202.3	1468
8b	Ru	143.8	287.1	1229
9	Mo	197.8/183.0	–	–
10b	Ru	161.5	279.1	1255
11b	Ru	159.5	281.9	1261
13b	Ru	159.8	281.8	1247
14b	Ru	160.6	281.8	1248
15b	Ru	161.7	281.5	1239
16b	Ru	165.3	280.8	1245
17b	Ru	170.0	279.5	1242
18b	Ru	168.3	278.7	1257
19	Ru	177.9	294.3	1217
20b	Pt	99.0	232.7	1242
21b	Pt	96.6	–	1259
22b	Pt	110.5	222.7	1262
23d	U	265.8	–	–
24a	Mg	177.2, 246.7 ^[a]	271.0	1327 ^[b]
24b	Mg	175.0	271.4	–
24c	Mg	162.9	–	1316
24d	Mg	173.3, ^[c] 167.7 ^[d]	–	1325
26	Ge	106.4	–	–
27	Sn	122.4	–	1321
28	Co	345.4	–	1306
29	Au	84.1	247.7	1342
33	Pt	111.2	–	–
34	Pt	41.4	–	–
35	Au	246.0	280.3	1125
36	Au	94.7	–	1175
37	Au	48.5	–	1186
41a	Ru	135.4	–	1249
41b	Ru	132	265.5	1250
41c	Ru	140	–	–
42	Ru	154	265	1242
43	Ru	181.3	249	1261

[a] solvent free, [b] calculated, [c] major product, [d] minor product.

Table 2: Selected crystallographic data.

compound	core metal	C≡P [Å]	M–CP [Å]	M–C–P [°]
4a	Pt	–	–	–
6a	Pt	1.666(6)	1.950(6)	144.0(3)
7	B	1.563(10) ^[a]	–	–
8	Ru	1.573(2)	2.057(2)	177.9(1)
9	Mo	–	–	–
10b	Ru	1.57(1)	2.05(1)	171.9(7)
11b	Ru	1.544(4)	2.065(4)	172.3(2)
13b	Ru	–	–	–
14b	Ru	–	–	–
15b	Ru	1.493(3)	2.118(3)	177.8(2)
16b	Ru	1.549(19)	2.076(9) ^[b]	172.8(6)
17b	Ru	–	–	–
18b	Ru	–	–	–
19	Ru	1.392(8)	2.186(8)	165.5(5)
20b	Pt	–	–	–
21b	Pt	1.5625(18)	1.9743(18)	176.62(12)
22b	Pt	1.5553(12)	1.9890(12)	176.47(8)
23d	U	1.523(8)	2.579(7)	177.5(4)
24a	Mg	1.553(2)	2.118(2)	177.37(15)
24b	Mg	1.501(4)	2.160(4)	178.5(3)
24c	Mg	1.550(2)	2.166(2)	176.3(1)
24d	Mg	1.531(3)	2.144(3)	176.8(2)
26	Ge	–	–	–
27	Sn	1.542(4)	2.216(4)	179.2(2)
28	Co	1.506(4)	1.926(4)	178.3(3)
29	Au	1.552(6)	1.972(6)	178.0(5)
33	Pt	–	–	–
34	Pt	1.663(9)	1.952(9)	145.2(6)
35	Au	1.642(4)	1.992(4)	146.3(2)
36	Au	1.631(4)	1.976(4)	151.4(3)
37	Au	1.605(4)	1.991(4)	155.4(3)
41a	Ru	1.544(10)	1.901(9)	175.8(5)
41b	Ru	1.638(17)	1.687(16) ^b	177.4(10)
41c	Ru	–	–	–
42	Ru	1.572(4)	1.904(4)	178.9(2)
43	Ru	1.53(2)	2.06(2)	176.0(13)

[a] decomposition of the product, [b] disorder in the crystallographic structure of C≡P.

potential use of this species as a linker in coordination polymers. Since then, a number of different approaches have been developed for the synthesis of related compounds, including the first cyaphide transfer reagent [Mg-(^{Dipp}NacNac)(η¹-C≡P)(dioxane)]. This compound allows for Grignard-like reactivity and opens up salt-metathesis protocols for the synthesis of metal cyaphido complexes.

Having overcome the challenge of accessing cyaphido metal complexes, in recent years the increase in synthetically available compounds has allowed researchers to turn their attention to *understanding* the properties of the cyaphide ion. Experimental and theoretical findings strongly suggest that (C≡P)[−] is a strong σ-donor, in line with related valence isoelectronic species such as acetylides. It also possesses moderate-to-good π-acceptor properties when bonded to metal centers through the carbon atom. The uniqueness of the cyaphido ligand—when compared to its lighter analog cyanide—is the energetically low-lying nature of the degenerate π* LUMO and LUMO+1. These orbitals, and the occupied π-bonding HOMO−1 and HOMO−2 dictate that

the reactivity of metal cyaphido complexes is predominantly driven by the π-manifold and not the phosphorus lone pair. This has implications in the synthesis of extended solids, of course, but also with regard to the stability of metal cyaphido complexes. The increased reactivity of the C–P π-bonds means that metal cyaphido complexes will readily react with azides (in an inorganic “click” reaction) to generate triazaphospholes. This reactivity will also unquestionably influence other applications of metal cyaphido complexes. One can envision oligomerization and polymerization reactions of the C≡P triple bond to afford conjugated ligands which can be used to connect metal centers. As a suitable ligand with which to enable electronic communication between metals, there are innumerable opportunities for the design and synthesis of extended metal–organic framework structures related to that of Prussian Blue. Having tamed the reactivity of the cyaphide ion and developed methodologies for its transfer between metal centers, the coming years will unquestionably see the application of this ion as a building block and novel chemical precursor. What is clear at this stage is that exciting new discoveries await using C≡P[−] as a chemical reagent for the synthesis of novel molecules and materials.

Acknowledgements

PC gratefully acknowledges funding by the Deutsche Forschungsgemeinschaft (DFG, grant 438203135). ESY and JMG thank the University of Oxford, the EPSRC, and OxICFM CDT for financial support ESY: EP/S023828/1). HG thanks the ETH Zürich (grant ETH-36 17-2) and Swiss National Science Foundation (SNF 200020_181966) for continuous support. CM and TG thank Freie Universität Berlin and the Deutsche Forschungsgemeinschaft (DFG) for generous financial support. The authors thank Mrs. Indira Kayumova for creating the front cover. Open Access funding enabled and organized by Projekt DEAL.

Conflict of Interest

The authors declare no conflict of interest.

Keywords: Coordination Chemistry · Cyaphide Ion · Phosphorus · π-Complexes · σ-Complexes

- [1] R. Appel, F. Knoll, I. Ruppert, *Angew. Chem. Int. Ed. Engl.* **1981**, *20*, 731–744.
- [2] J. F. Nixon, *Chem. Rev.* **1988**, *88*, 1327–1362.
- [3] J. M. Goicoechea, H. Grützmacher, *Angew. Chem. Int. Ed.* **2018**, *57*, 16968–16994.
- [4] A. L. Colebatch, B. J. Frogley, A. F. Hill, C. S. Onn, *Chem. Eur. J.* **2021**, *27*, 5322–5343.
- [5] N. T. Coles, A. Sofie Abels, J. Leitzl, R. Wolf, H. Grützmacher, C. Müller, *Coord. Chem. Rev.* **2021**, *433*, 213729.
- [6] R. Appel, F. Knoll, *Adv. Inorg. Chem.* **1989**, *33*, 259–361.
- [7] L. N. Markovski, V. D. Romanenko, *Tetrahedron* **1989**, *45*, 6019–6090.

- [8] M. Regitz, *Chem. Rev.* **1990**, *90*, 191–213.
- [9] L. Weber, *Eur. J. Inorg. Chem.* **2000**, 2425–2441.
- [10] F. Mathey, *Angew. Chem. Int. Ed.* **2003**, *42*, 1578–1604.
- [11] P. Le Floch, *Coord. Chem. Rev.* **2006**, *250*, 627–681.
- [12] C. Müller, D. Vogt, *Dalton Trans.* **2007**, 5505–5523.
- [13] C. Müller, L. E. E. Broeckx, I. De Krom, J. J. M. Weemers, *Eur. J. Inorg. Chem.* **2013**, 187–202.
- [14] B. W. Shober, W. F. Spanutius, *Early Publications of the Lehigh Faculty* **1894**, 229–232.
- [15] F. F. Puschmann, D. Stein, D. Heift, C. Hendriksen, Z. A. Gal, H. F. Grützmacher, H. Grützmacher, *Angew. Chem. Int. Ed.* **2011**, *50*, 8420–8423.
- [16] G. Becker, W. Schwarz, N. Seidler, M. Westerhausen, *Z. Anorg. Allg. Chem.* **1992**, *612*, 72–82.
- [17] G. Herzberg, *Nature* **1930**, *126*, 131–132.
- [18] M. Guelin, J. Cernicharo, G. Paubert, B. E. Turner, M. Guelin, J. Cernicharo, G. Paubert, B. E. Turner, *Astron. Astrophys.* **1990**, *230*, L9–L11.
- [19] M. Agúndez, J. Cernicharo, M. Guélin, *Astrophys. J.* **2007**, *662*, L91–L94.
- [20] S. N. Milam, D. T. Halfen, E. D. Tenenbaum, A. J. Apponi, N. J. Woolf, L. M. Ziurys, *Astrophys. J.* **2008**, *684*, 618–625.
- [21] T. E. Gier, *J. Am. Chem. Soc.* **1961**, *83*, 1769–1770.
- [22] J. K. Tyler, *J. Chem. Phys.* **1964**, *40*, 1170.
- [23] M. J. Hopkinson, H. W. Kroto, J. F. Nixon, N. P. C. Simmons, *J. Chem. Soc. Chem. Commun.* **1976**, 513–515.
- [24] M. J. Hopkinson, H. W. Kroto, J. F. Nixon, N. P. C. Simmons, *Chem. Phys. Lett.* **1976**, *42*, 460–461.
- [25] H. W. Kroto, J. F. Nixon, N. P. C. Simmons, *J. Mol. Spectrosc.* **1979**, *77*, 270–285.
- [26] G. Becker, G. Gresser, W. Uhl, *Z. Naturforsch. B* **1981**, *36*, 16–19.
- [27] G. Becker, W. Becker, R. Knebl, H. Schmidt, U. Hildenbrand, M. Westerhausen, *Phosphorus Sulfur Relat. Elem.* **1987**, *30*, 349–352.
- [28] K. S. Pitzer, *J. Am. Chem. Soc.* **1948**, *70*, 2140–2145.
- [29] R. S. Mulliken, *J. Am. Chem. Soc.* **1950**, *72*, 4493–4503.
- [30] P. Pyykkö, Y. Zhao, *Mol. Phys.* **1990**, *70*, 701–714.
- [31] H. Jun, V. G. Young, R. J. Angelici, *J. Am. Chem. Soc.* **1992**, *114*, 10064–10065.
- [32] M. T. Nguyen, T. K. Ha, *J. Mol. Struct. (Theochem)* **1986**, *139*, 145–152.
- [33] M. T. Nguyen, L. Landuyt, L. G. Vanquickenborne, *J. Org. Chem.* **1993**, *58*, 2817–2821.
- [34] S. Creve, M. T. Nguyen, L. G. Vanquickenborne, *Eur. J. Inorg. Chem.* **1999**, 1281–1289.
- [35] M. Hofmann, P. Von, R. Schleyer, M. Regitz, *Eur. J. Org. Chem.* **1999**, 3291–3303.
- [36] C. Beck, R. Schinke, J. Koput, *J. Chem. Phys.* **2000**, *112*, 8446.
- [37] V. F. Kalasinsky, S. Pechsiri, *J. Raman Spectrosc.* **1985**, *16*, 190–192.
- [38] J. W. C. Johns, J. M. R. Stone, G. Winnewisser, *J. Mol. Spectrosc.* **1971**, *38*, 437–440.
- [39] S. P. Anderson, H. Goldwhite, D. Ko, A. Letsou, F. Esparza, *J. Chem. Soc. Chem. Commun.* **1975**, 744–745.
- [40] J. B. Robert, H. Marsmann, I. Absar, J. R. Van Wazer, *J. Am. Chem. Soc.* **1971**, *93*, 3320–3325.
- [41] K. Hübler, P. Schwerdtfeger, *Inorg. Chem.* **1999**, *38*, 157–164.
- [42] M. F. Lucas, M. C. Michélini, N. Russo, E. Sicilia, *J. Chem. Theory Comput.* **2008**, *4*, 397–403.
- [43] P. Dréan, J. Demaison, L. Poteau, J. M. Denis, *J. Mol. Spectrosc.* **1996**, *176*, 139–145.
- [44] O. Mó, M. Yáñez, J. Guillemin, E. H. Riague, J. Gal, P. Maria, C. D. Poliart, *Chem. Eur. J.* **2002**, *8*, 4919–4924.
- [45] G. Pascoli, H. Lavendy, *J. Phys. Chem. A* **1999**, *103*, 3518–3524.
- [46] All calculations were carried out with the ORCA program package. Unless stated otherwise, all calculations were carried out on isolated molecules (in the gas phase). Density fitting techniques, also called resolution-of-identity approximation (RI), were used for GGA calculations and the RIJCOSX approximation was used for CASSCF calculations. Atom-pairwise dispersion corrections with the Becke-Johnson damping (D3BJ) were used for all DFT calculations. Orbital pictures were rendered with the software Chimera. The geometry and molecular orbitals of the cyanide and cyaphide anions were obtained using TPSS-D3BJ/def2-TZVP. Geometries and frequencies of the coordination compounds were obtained using B97-3c. EDA-NOCV calculations and IBO calculations for the silver complexes were carried out using TPSS-D3BJ/ZORA-def2-TZVP (old-ZORA-TZVP on Ag). The same method was used to analyse the electronic structure of Ru₂CP, whereas a CASSCF calculation consisting of 19 electrons in 14 orbitals was carried out to analyse the electronic structure of Ru₂CN.
- [47] H. Jun, V. G. Young, R. J. Angelici, *J. Am. Chem. Soc.* **1991**, *113*, 9379–9380.
- [48] L. Weber, I. Schumann, T. Schmidt, H.-G. Stämmler, B. Neumann, *Z. Anorg. Allg. Chem.* **1993**, *619*, 1759–1764.
- [49] H. Jun, R. J. Angelici, *Organometallics* **1994**, *13*, 2454–2460.
- [50] M. Finze, E. Bernhardt, H. Willner, C. W. Lehmann, *Angew. Chem. Int. Ed.* **2004**, *43*, 4160–4163.
- [51] P. B. Hitchcock, M. J. Maah, J. F. Nixon, J. A. Zora, G. J. Leigh, M. A. Bakar, *Angew. Chem. Int. Ed. Engl. Angew. Chem. Int. Ed.* **1987**, *26*, 474–475.
- [52] P. B. Hitchcock, M. Amélia, N. D. A. Lemos, M. F. Meidine, J. F. Nixon, A. J. L. Pombeiro, *J. Organomet. Chem.* **1991**, *402*, C23–C26.
- [53] J. G. Cordaro, D. Stein, H. Rügger, H. Grützmacher, *Angew. Chem. Int. Ed.* **2006**, *45*, 6159–6162.
- [54] A. Ehlers, J. G. Cordaro, D. Stein, H. Grützmacher, *Angew. Chem. Int. Ed.* **2007**, *46*, 7878–7881.
- [55] S. M. Mansell, M. Green, C. A. Russell, *Dalton Trans.* **2012**, *41*, 14360–14368.
- [56] N. Trathen, M. C. Leech, I. R. Crossley, V. K. Greenacre, S. M. Roe, *Dalton Trans.* **2014**, *43*, 9004–9007.
- [57] M. C. Leech, I. R. Crossley, *Dalton Trans.* **2018**, *47*, 4428–4432.
- [58] S. K. Furfari, M. C. Leech, N. Trathen, M. C. Levis, I. R. Crossley, *Dalton Trans.* **2019**, *48*, 8131–8143.
- [59] L. D. Field, A. M. Magill, T. K. Shearer, S. J. Dalgarno, P. Turner, *Organometallics* **2007**, *26*, 4776–4780.
- [60] M. C. Levis, K. G. Pearce, I. R. Crossley, *Inorg. Chem.* **2019**, *58*, 14800–14807.
- [61] J. J. Garcia, W. D. Jones, *Organometallics* **2000**, *19*, 5544–5545.
- [62] C. Müller, C. N. Iverson, R. J. Lachicotte, W. D. Jones, *J. Am. Chem. Soc.* **2001**, *123*, 9718–9719.
- [63] H. Petzold, T. Weisheit, H. Görls, H. Breitzke, G. Buntkowsky, D. Escudero, L. González, W. Weigand, *Dalton Trans.* **2008**, 1979–1981.
- [64] D. Escudero, M. Assmann, A. Pospiech, W. Weigand, L. González, *Phys. Chem. Chem. Phys.* **2009**, *11*, 4593–4600.
- [65] D. Escudero, T. Weisheit, W. Weigand, L. González, *Dalton Trans.* **2010**, *39*, 9505–9513.
- [66] T. Görlich, D. S. Frost, N. Boback, N. T. Coles, B. Dittrich, P. Müller, W. D. Jones, C. Müller, *J. Am. Chem. Soc.* **2021**, *143*, 19365–19373.
- [67] a) P. Hofmann, G. Unfried, *Chem. Ber.* **1992**, *125*, 659; b) C. Massera, G. Frenking, *Organometallics* **2003**, *22*, 2758.
- [68] C. J. Hoerger, F. W. Heinemann, E. Louyriac, L. Maron, H. Grützmacher, K. Meyer, *Organometallics* **2017**, *36*, 4351–4354.
- [69] D. Heift, Z. Benkő, H. Grützmacher, *Dalton Trans.* **2014**, *43*, 5920–5928.
- [70] S. P. Green, C. Jones, A. Stasch, *Science* **2007**, *318*, 1754–1757.
- [71] D. W. N. Wilson, D. D. L. Jones, C. D. Smith, M. Mehta, C. Jones, J. M. Goicoechea, *Dalton Trans.* **2022**, *51*, 898–903.

- [72] M. Ma, A. Stasch, C. Jones, *Chem. Eur. J.* **2012**, *18*, 10669–10676.
- [73] D. W. N. Wilson, S. J. Urwin, E. S. Yang, J. M. Goicoechea, *J. Am. Chem. Soc.* **2021**, *143*, 10367–10373.
- [74] W. P. Fehlhammer, M. Fritz, *Chem. Rev.* **1993**, *93*, 1243–1280.
- [75] T. Görlich, C. Müller, unpublished results.
- [76] J. C. T. R. Burckett-St. Laurent, P. B. Hitchcock, H. W. Kroto, M. F. Meidine, J. F. Nixon, *J. Organomet. Chem.* **1982**, 238, C82–C84.
- [77] P. Pyykkö, M. Atsumi, *Chem. Eur. J.* **2009**, *15*, 12770–12779.
- [78] E. S. Yang, J. M. Goicoechea, *Angew. Chem. Int. Ed.* **2022**, *61*, e202206783.
- [79] W. V. Konze, V. G. Y. Young, R. J. Angelici, *Organometallics* **1999**, *18*, 258–267.
- [80] J. A. W. Sklorz, C. Müller, *Eur. J. Inorg. Chem.* **2016**, 2016, 595–606.
- [81] J. A. W. Sklorz, S. Hoof, N. Rades, N. Derycke, L. Könczöl, D. Szieberth, M. Weber, J. Wiecko, L. Nyulászi, M. Hissler, C. Müller, *Chem. Eur. J.* **2015**, *21*, 11096–11109.

Manuscript received: December 1, 2022

Accepted manuscript online: January 10, 2023

Version of record online: May 15, 2023